JPL PUBLICATION 80-54

(NASA-CR-163564) TECHNIQUES FOR MEASURING ARRIVAL TIMES OF PULSAR SIGNALS 1: DSN OBSERVATIONS FROM 1968 TO 1980 (Jet Propulsion Lab.) 88 p HC A05/MF A01 CSCL 03A G3/89

N80-33317

Unclas 28761

# Techniques for Measuring Arrival Times of Pulsar Signals I: DSN Observations from 1968 to 1980

G.S. Downs
P.E. Reichley

August 15, 1980



National Aeronautics and
Space Administration

Jet Propulsion Laboratory
California Institute of Technology
Pasadena, California

JPL PUBLICATION 80-54

# Techniques for Measuring Arrival Times of Pulsar Signals I: DSN Observations from 1968 to 1980

G.S. Downs
P.E. Reichley

August 15, 1980

National Aeronautics and
Space Administration

Jet Propulsion Laboratory
California Institute of Technology
Pasadena, California

# ABSTRACT

Natural radio emissions from pulsating radio sources (pulsars) have been detected at Goldstone on a regular basis since 1968. Scientific analysis of these signals has stimulated ideas of traversing the interplanetary medium and beyond, to the "home" of comets, using these natural beacons as navigation aids. Therefore, the techniques used in the ground-based observations of pulsars are described here in the required detail, many of them being directly applicable in a navigation scheme. The arrival times of the pulses intercepting Earth are measured at time intervals varying from a few days to a few months. Low-noise, wide-band receivers, unique to the stations of NASA's Deep Space Network, amplify signals intercepted by the 26-m, and 34-m, and 64-m antennas at Goldstone and in Spain. Digital recordings of total received signal power versus time are cross correlated with the appropriate pulse template, thereby providing an estimate of the pulse arrival time relative to the station clock. Corrections are applied to the station clock to obtain arrival times relative to ephemeris time. Drifts in phase encountered during signal integration are removed. The arrival times are then referred to the barycenter of the solar system for scientific studies, and to the geocenter for export to other investigators.

CONTENTS



PRECEDING PAGE BLANK NOT FILMED

Figures

Figures

Figures



Tables

Tables

## SECTION I

## INTRODUCTION

Natural sources of pulsating radiation were first observed in 1967 (Refs. 1, 2) by radio astronomers at Cambridge University in England. These pulsating radio sources (pulsars) are exciting because they (1) are thought to represent a stage in stellar evolution known as neutron stars (Ref. 3), providing a probe of an extremely dense state of matter; (2) exhibit changing, often dramatically so, behavior in the pulse period, signifying changes in the spin rate of the neutron star driving the pulse generating mechanism; and (3) have large space velocities, implying violent origins.

A series of measurements is being established using the NASA–JPL Deep Space Network (DSN) which will allow a probing of the neutron star interior and a direct measurement of changes in spin rate and angular motion. The purpose of the measurements is to measure the phase of the pulse train at known epochs. It requires little imagination to realize that the simultaneous comparison of the phase of a pulse train at two different DSN stations represents either a measurement of the difference between the station clocks, or a measurement of the location of one station relative to the other. In navigation, one assumes the clocks are synchronized. Differences in pulse phase are then attributed to differences in location. We need only to replace one DSN station with a spacecraft to complete the illustration.

The purpose of this report is to describe in appropriate detail the techniques used currently in the DSN for measuring the arrival time of a particular pulse (alternatively, the phase of the pulse train relative to a given epoch). Phase measurements were begun in September 1968 and continue to the present. The 24 pulsars included in this series are listed in Table 1 with appropriate dates on which measurements began. An example of the results of this long series of measurements is presented in Table 7.

Many characteristics of the pulsars have been or can be deduced from the measurement of pulse phase at a series of epochs if the epochs occur often enough (weekly to monthly) and over a sufficient time span (years). Usually a parameterized model of the pulsar is constructed which is used to predict the time-of-arrival of a given pulse (or the phase of the pulse train at a given epoch). The parameters are then adjusted to minimize the mean square difference between the predictions and the measurements. The final values of the model parameters are dependent on the planetary ephemeris used in the data reduction, since all observations are usually referred to the barycenter of the solar system. The importance of this is clear when one realizes that 2 milli-seconds flight time in the displacement of the barycenter amounts to as much as 1 arc-second displacement in the position of the pulsar. Errors in the knowledge of the barycenter with time scales of tens of years are caused by inaccuracies in the values of the masses of the outer planets. These slow curvilinear errors affect the values of the higher-order derivatives of the pulse period. Hence, though all current ephemerides may produce similar pulsar model parameters, improved ephemerides available twenty years from now will produce significantly different results. Tables of geocentric arrival times, being important

Table 1. 24 Pulsars Monitored at JPL at Frequencies of 2295 MHz and 2388 MHz

| Entry | Pulsar | Start Date |
|---|---|---|
| 1 | 0031-07 | 5 Mar 1970 |
| 2 | 0329+54 | 5 Sep 1968 |
| 3 | 0355+54 | 5 May 1973 |
| 4 | 0525+21 | 1 Jun 1969 |
| 5 | 0628-28 | 30 Dec 1969 |
| 6 | 0736-40 | 1 Oct 1970 |
| 7 | 0823+26 | 12 Feb 1969 |
| 8 | 0833-45 | 22 Nov 1968 |
| 9 | 0950+08 | 5 Sep 1968 |
| 10 | 1133+16 | 25 Oct 1968 |
| 11 | 1237+25 | 10 Aug 1969 |
| 12 | 1604-00 | 1 Oct 1970 |
| 13 | 1642-03 | 12 Jul 1969 |
| 14 | 1706-16 | 1 Oct 1970 |
| 15 | 1749-28 | 2 May 1969 |
| 16 | 1818-04 | 29 Dec 1969 |
| 17 | 1911-04 | 5 Mar 1970 |
| 18 | 1929+10 | 29 Jun 1969 |
| 19 | 1933+16 | 23 Dec 1968 |
| 20 | 2016+28 | 5 Sep 1968 |
| 21 | 2021+51 | 30 Dec 1969 |
| 22 | 2045-16 | 10 Dec 1968 |
| 23 | 2111+46 | 30 Dec 1969 |
| 24 | 2217+47 | 30 Dec 1969 |

archives of pulsar behavior, are independent of small changes in the ephemerides of the planets. They form the exported form of the observational results.

The measurements were performed earlier at a frequency of 2388 MHz on the 26-m antenna at Deep Space Station 13 (DSS 13) and the 64-m antenna at DSS 14. Current observations are at 2295 MHz, utilizing all facilities at Goldstone and in Spain. Detected pulsar signals are sampled, integrated and recorded on magnetic tape. Data collection and recording is discussed in Section II. The data are then edited and, for the early years, collated according to the pulsar, as described in Section III. The collated data, stored on magnetic tapes, was used to derive a template for each pulsar, representing the average power level across a pulse of radiation. The template is then cross correlated with each data record of the particular pulsar to obtain an estimate of the pulse arrival time. The procedures used in constructing the templates is described in Section IV and the cross correlation process is discussed in Section V. The correction of the arrival time estimates for various small effects is discussed in Section VI. A sample list of geocentric times-of-arrival is presented in Section VII.

## SECTION II

## DATA COLLECTION

### A. RECEIVING, DETECTION, AND RECORDING

It was shown shortly after the discovery of pulsars that they could be detected at 2295 MHz (Ref. 4). Shortly thereafter, in August 1968, JPL observations at 2388 MHz were begun using the 26-m antenna of DSS 13 at the Goldstone complex. The wide bandwidths (about 12 MHz) and the low system temperatures (about 16 K) allowed detection of three of the first four pulsars discovered. Over the following months the observations have been expanded to include 24 objects, utilizing all antennas at Goldstone and Madrid.

The receiver consists of the antenna, a right circularly polarized feed horn (left circularly polarized at 2388 MHz), and a maser preamplifier followed by conversion to and amplification at intermediate frequencies (IF). Low-loss cabling then carries the signal to the receiver room for more IF amplification. The receiver bandwidth is limited to 12 MHz by either the IF portion of the receiver or by a filter inserted for that purpose. Square-law detection of the signal is then performed, followed by low-pass filtering. The output of the low-pass filter is amplified by a wideband DC amplifier to a 1- to 2-volt level. Subsequently, the signal is converted to digital form in a sampling process. The integration time (see Ref. 5 for a definition) of the post-detection filter is chosen to match the time interval between analog-to-digital (A/D) conversions.

The data processing, from sampling to the dumping onto magnetic tape, is under computer control. The detected signal is sampled at a rate equal to 5000 times the apparent pulse period, corresponding to sample intervals of 50 μsec up to 800 μsec. Converted to a digital signal by an A/D converter, the samples are stored in the memory of an SDS 930 computer or a standard station Modcomp computer. Data samples are superimposed modulo the pulse period. Samples from 500 pulse periods are superimposed congruently. Then a 5000-word array representing the superposition of 500 pulses is dumped onto tape. This accumulation of pulses continues until (a) detection is ensured, or (b) it is clear the pulses are too weak at this time to be observed. Accumulations rarely run more than one hour.

The form of the recorded data is sketched in Figure 1. The pulse is sitting on top of a system noise power corresponding to a temperature $T_s$. The peak equivalent temperature of the pulse is $T_p$. The 5000 samples spanning one pulse period are plotted from left to right. The time of the first data sample, plotted at the left, corresponds to a particular epoch of Universal Time (UT) as recorded at the station. This start time is recorded in UT (station). The train of received pulses then has a particular phase relative to the start time. The pulse train is folded in upon itself to beat down the effects of receiver noise fluctuations. Rather than think in terms of the phase of the pulse train, we ask for the arrival time of the first pulse after the start time. Hence, the pulse delay is added to the UT (station) epoch corresponding to the start time to yield an epoch for the arrival time of the pulse.

The phase of the pulse train may not remain constant during the superposition of many pulses. The subsequent drift in phase requires that a correction be applied to the measured pulse delay. This

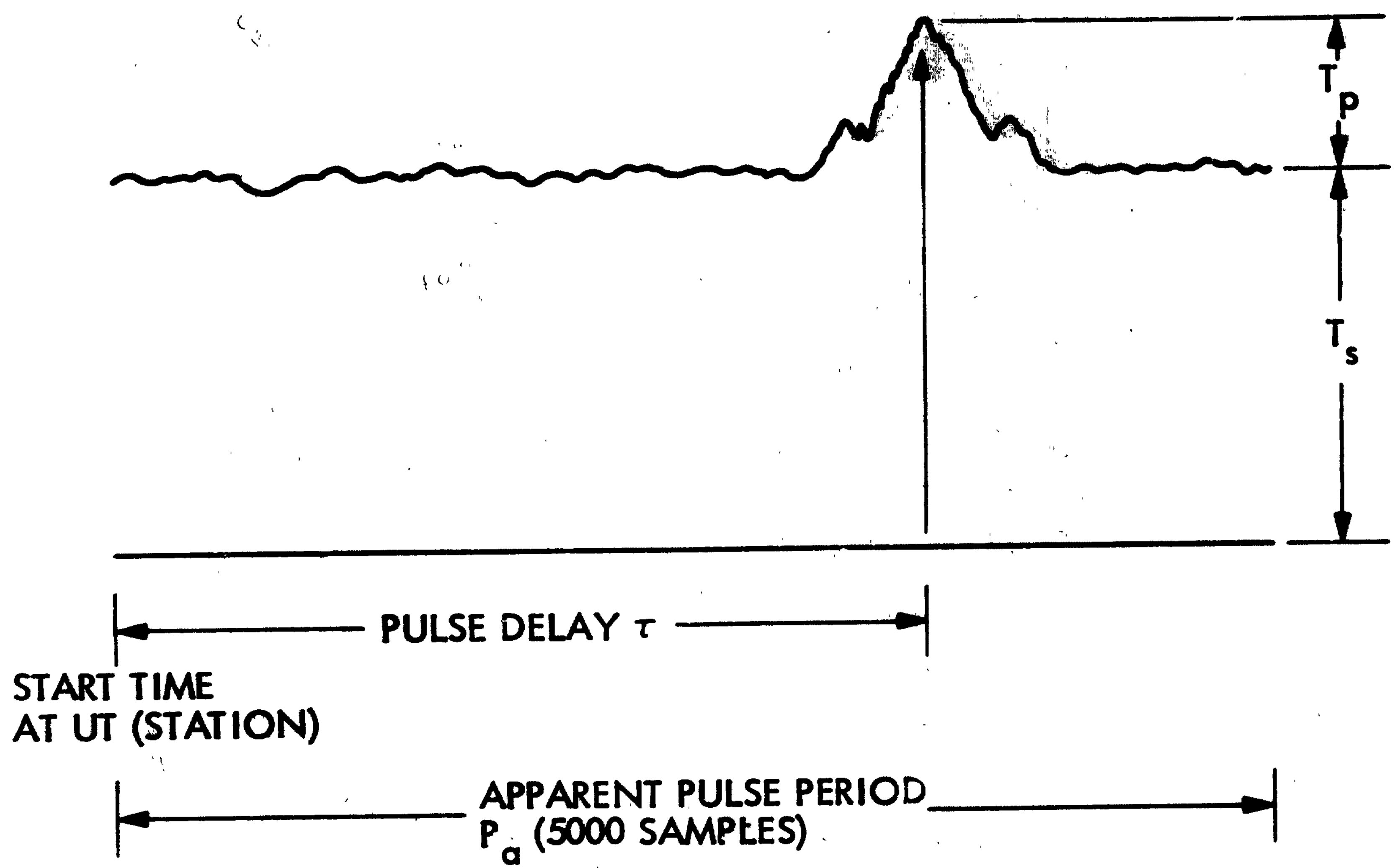


Figure 1. Nomenclature of the Pulsed Emission

correction is discussed in Section VI, D. Small corrections are required in the start time and in the UT (station) defined by a particular clock. These corrections are discussed in this section and in Section VI.

B. THE SYSTEM CONFIGURATION CODES

The measurement system is shown diagrammatically in Figure 2. The experimental hardware is grouped into units defined by the dashed boxes. Each subsystem so defined has been interchanged with other similar subsystems, causing significant changes in the measured phases. Hence, a system configuration code has been constructed to alert the analyst to changes in the system. The code varies from 0 to 21, representing 22 significantly distinct combinations of antenna, receiver, observing frequency, computer, data collection controller, and station clock. A summary of the basic configurations (0-5) and (17-21) appears in Table 2. Additional configuration codes (6-16) were created to denote the use of an observing frequency of 2295 MHz or 2328 MHz, and their relationship to the basic codes are shown in Table 3. Left circular polarization (LCP) is to be assumed unless specified as right circular polarization (RCP).

Since the system configurations do not change in principle from one to the other, only configuration 0 is described in detail. Highlights of the other configurations are noted in the following paragraphs. Configuration 0 includes the 26-m antenna at DSS 13. The radio frequency bandpass is determined by the IF amplifiers. The final IF amplification, detection, and low-pass filtering is done by a receiver (labeled as receiver 1) built in 1968 by C. F. Foster. The timing control box was designed by G. A. Morris and is labeled timer 1.

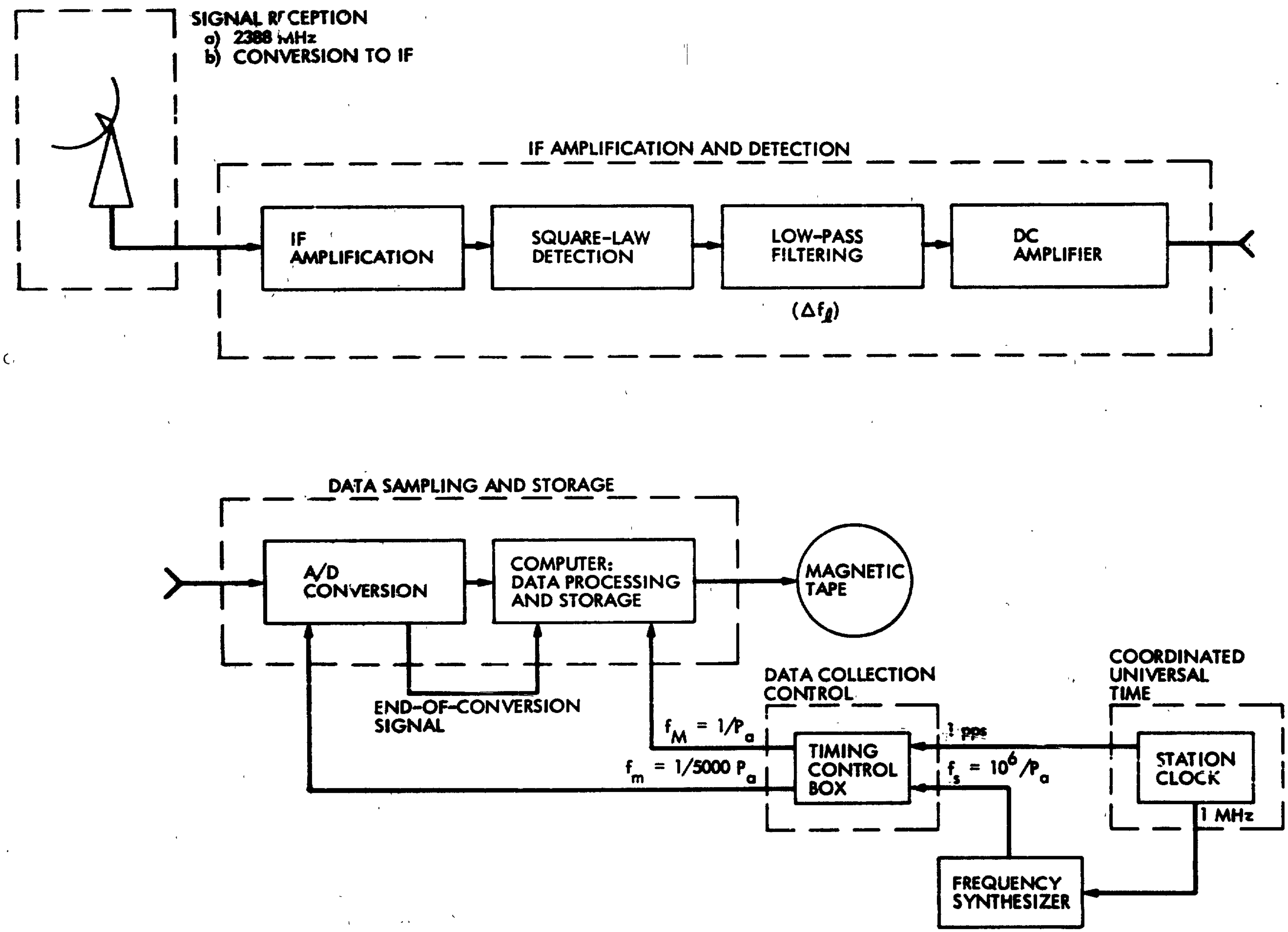


Figure 2. The Receiving, Detection, and Data Recording of Signals from Pulsars

Table 2. Chronology of the Major Experiment Configurations for Collecting Pulsar Timing Data

| Configuration Code | Station | Dates In Effect (d/m/yr) | Description |
|---|---|---|---|
| 0 (early) | DSS 13 | 05/09/68-10/01/74 | 26-m Antenna; Receiver 1; Timer 1; 1-sec Tick Derived From Ce Frequency Standard; Slow A/D Converter |
| 0 (late) | DSS 13 | 10/01/74-01/04/76 | Changed From Receiver 1 to 2 |
| 4 | DSS 13 | 01/04/76-Present | Changed from Timer 1 to 3 |
| 1 | DSS 14 | 05/09/68-14/04/73 | Receiver 1 Plus 12-MHz IF Filter; Fast A/D Converter |
| 2 | DSS 14 | 14/04/73-01/11/74 | Changed From Timer 1 to 2 |
| 3 | DSS 14 | 01/11/74-01/04/76 | 1-sec Pulse Widened From 100 μsec to 200 μsec; -0.996550 Seconds Added to Start Epoch if Julian Date > 2442460.5 |
| 5 | DSS 14 | 01/04/76-Present | Timer 2 Replaced With Timer 1 |
| 17 | DSS 62 | 01/04/79-Present | 2295 MHz, RCP, using station TPA with Modcomp |
| 18 | DSS 11 | 01/12/79-Present | 2295 MHz, RCP, using station TPA with Modcomp |
| 19 | DSS 63 | 01/11/79-Present | 2295 MHz, RCP, using station TPA with Modcomp |
| 20 | DSS 12 | 01/04/80-Present | 2295 MHz, RCP, using station TPA with Modcomp |
| 21 | DSS 14 | 01/04/80-Present | 2295 MHz, RCP, using station TPA with Modcomp |

Table 3. The Configuration Codes Corresponding to Non-Standard Observing Frequencies

| Configuration | Configuration | Observing Frequency (MHz) | Description |
|---|---|---|---|
| 8 | 0 | 2328 | |
| 9 | | 2295 | |
| 10 | 1, 2, 3 | 2328 | |
| 11 | | 2295 | |
| 8 | 4 | 2328 | |
| 7 | | 2295 | |
| 6 | 5 | 2295 | |
| 12 | Any | | Denotes a correction w. s made to standard post-detection $\Delta f_\ell$ |
| 13 | 4 | 2295 | RCP |
| 14 | 5 | 2295 | RCP |
| 15 | 5 | 2295 | DSS 13 via link to DSS 14 |
| 16 | 5 | 2295 | DSS 12 via link to DSS 14 |

The relationship between the epoch-defining 1-second pulse and Universal Time as disseminated at the station, UT (station), is shown in Figure 3 along with the relationships for the other codes. Exact relations between UT (station) and Coordinated Universal Time (UTC) is discussed in Section VI. Data sampling in configuration codes less than 17 is performed by a 12-bit A/D converter with a 40 μsec conversion time. The samples are stored in an SDS 930 computer having a 16,384-word memory. The station telemetry processor assembly (TPA) is used in codes 17 or larger.

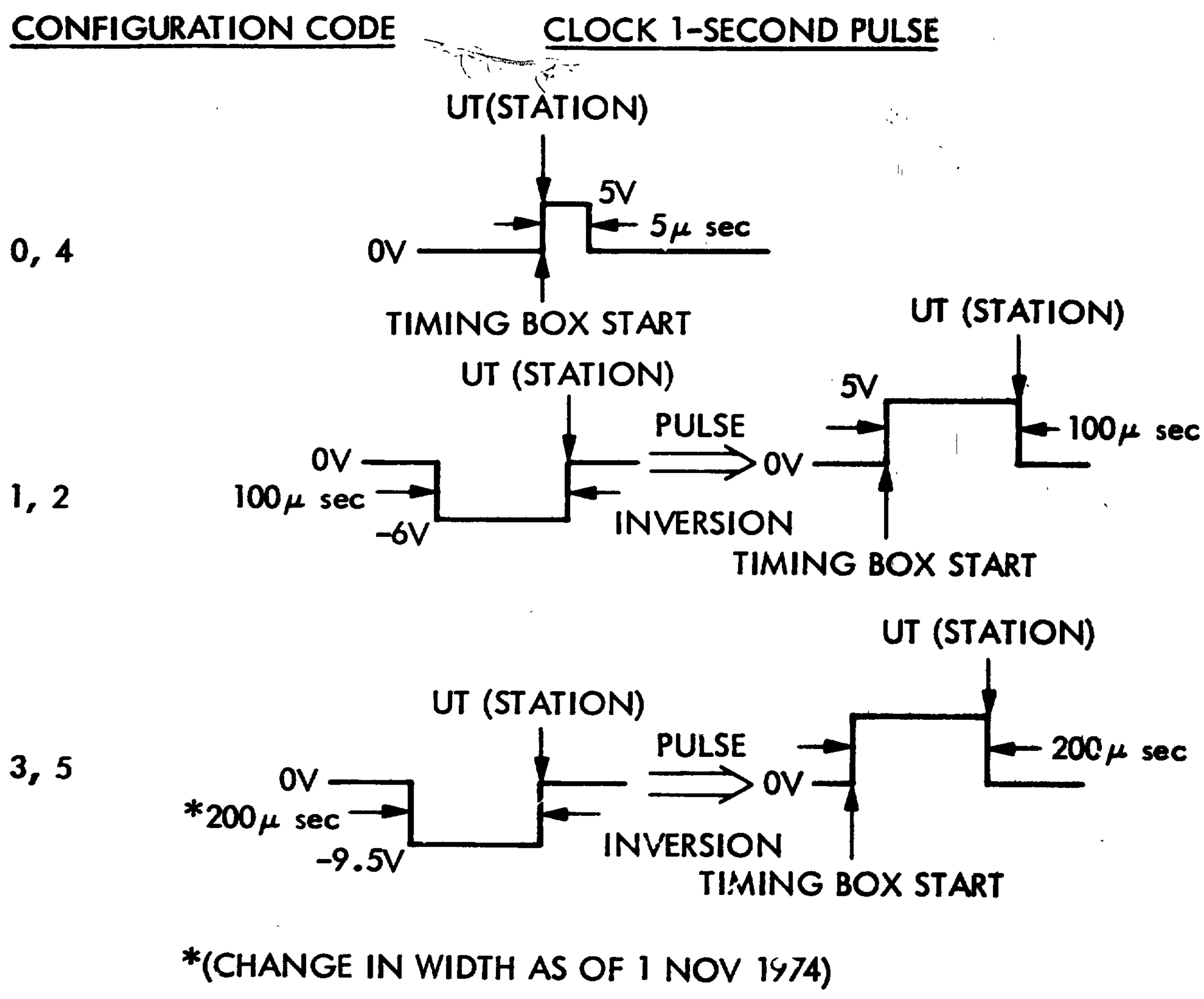


**Figure 3.** The 1-Second Pulses from the Station Clocks at DSS-13 and DSS-14, Goldstone, and Their Relation to UT (station)

The final IF amplification and detection is performed in the steps shown in Figure 2. The first unit built was transported between DSS 13 and DSS 14 until 10 Jan. 1974, when it was permanently installed at DSS 14. This unit was replaced at DSS 13 by a programmable unit built by C. F. Foster (described in Ref. 6 and labeled receiver 2). This change is not noted by a configuration code change. Hence, code 0 consists of an early phase (pre-10 Jan. 1974, Julian date 2442057.5) and a late phase (post-10 Jan. 1974).

The timing control box used here is not described elsewhere, so a block diagram is presented here for tutorial purposes. Other control boxes used in other configurations operate on the same principle, but differ in complexity and detail. Careful study of Figure 4 shows that a string of fast and slow pulses are generated by the timing control box to control the data sampling. The pulses are derived by counting down pulses from a frequency synthesizer, starting at a well-defined time by gating the synthesizer output. The gate must be armed and then a 1-sec pulse must be received before counting begins. To assist the operator in determining on which second the counting started, the 1-sec pulses are counted down by 10 so that counting will start modulo 10 seconds.

The fast pulses, occurring every $P_a/5000$ seconds, where $P_a$ is the apparent pulse period, are used to strobe the A/D converter. The slower pulses, occurring every $P_a$ seconds, are used to control the data transfer into core memory. On the first slow pulse, a computer interrupt is coincident with the slow pulse commands the A/D converter to begin operation. About 20 μsec later the end-of-convertion (EOC) interrupt forces the computer to accept the new word, and about 20 μsec after

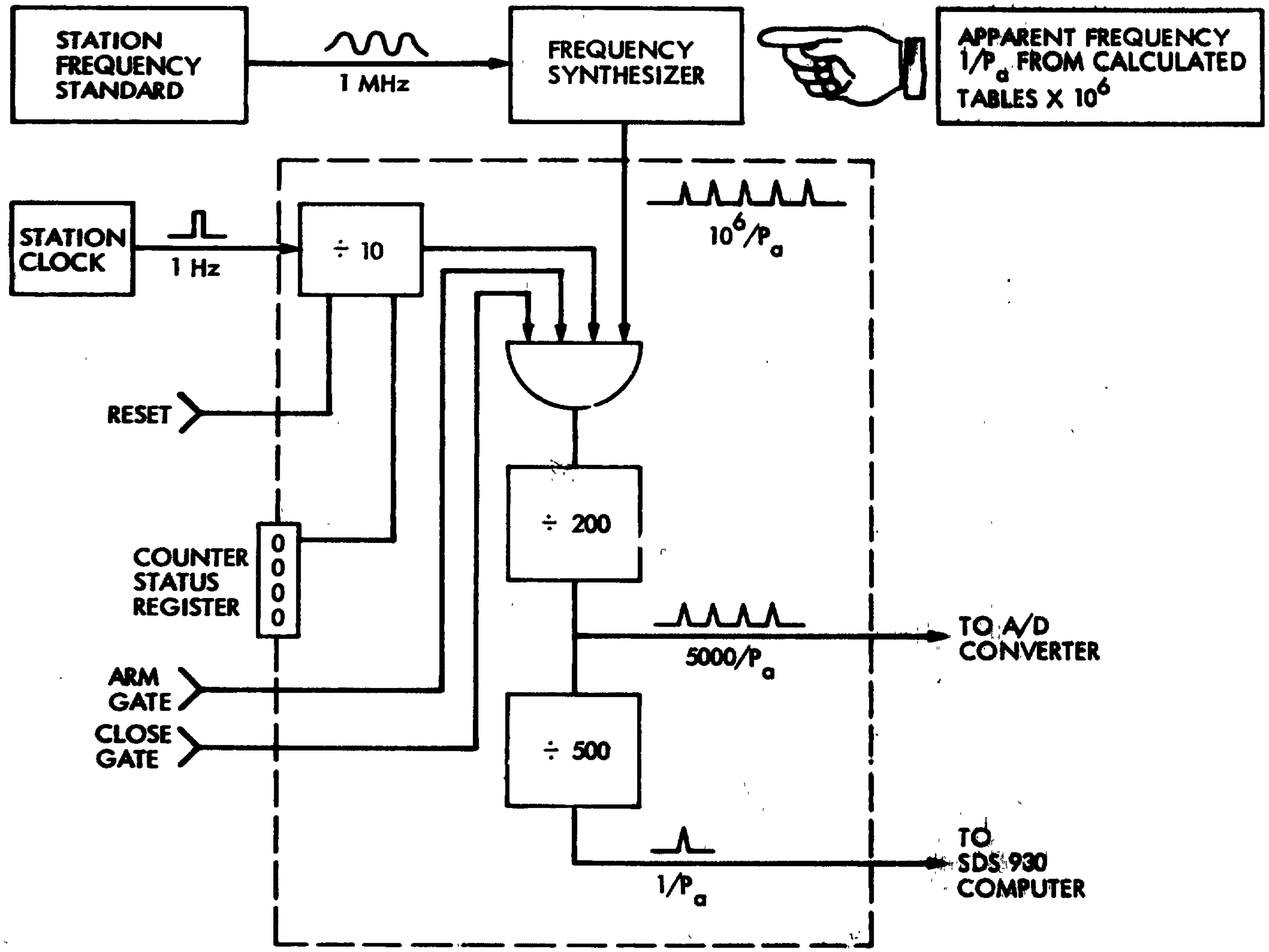


Figure 4. The Timing Control Box for Pulsar Data Collection

interruption, the word has been added to the proper memory location. Note that although it takes time to set up the computer to accept data, the EOC pulse arrives after the setup, so the first sample accepted is, in fact, coincident in time with the 1-sec pulse modulo one pulse period. However, a configuration exists in which the first sample is <u>not</u> coincident, and a correction must be applied.

The data sampling and superposition is under the control of a program written by G. A. Morris. The program also controlled the writing of the results onto magnetic tape for further reduction.

The apparent period $P_a$ is the result of the Doppler effect caused by Earth's motion about the barycenter of the solar system. Tables of $P_a$ are computed using a barycentric ephemeris of Earth and a crude but adequate model of the pulsar. The model includes the celestial coordinates of the object as well as the barycentric model of the pulse period (usually a period $P_0$ at some epoch $t_0$, and the first derivative $\dot{P}_0$). The values of $P_a$ are tabulated at 15-minute intervals between rise and set for any given day. The operator then chooses the value corresponding to the middle of the intended interval of pulse integration.

Configuration 1 consists of the 64-m antenna at DSS 14, the same IF amplification and detection unit, and the same timing box used in the early configuration 0. A 12-MHz IF filter is added to the chain to limit the IF bandwidth. The computer is again the SDS 930. The A/D converter, however, responds within 5 μsec of being strobed with a convert command. The computer, requiring about 20 μsec to arm the interrupt and start the data flow, misses the first data sample. The data stream is then shifted $P_a/5000$ seconds later in time. This shift is as large as 0.8 msec and is added to the UT (station) recorded by the operator.

Timer 1 was designed to accept the rising edge of a positive 1-sec pulse as the definition of UT (station). The 1-sec pulse distributed at DSS 14 is negative-going, the rising edge being coincident with UT (station). The necessary pulse inversion then causes the timing box to begin counting earlier than intended by a time equal to the width of the 1-sec pulse. This amounts to 100 μsec in configuration 1 and 200 μsec in configurations 3 and 5.

A programmable timing box, designed, built, and programmed by A. G. Slekys (Ref. 7) replaced the original timing box at DSS 14. This timer is labeled timer 2, and pertains to codes 2 and 3. A failure occurred in timer 2 which caused the start times of code 3 recorded between Julian dates 2442460.5 and 2443105.5 (17 Feb. 1975 and 23 Nov. 1976) to be earlier than intended. The correction is a subtraction of nearly 1 second. The exact correction was determined from a preliminary fit of a model of the pulsar emission times to the data. A correction of −0.996550 seconds to the start time aligned the affected arrival times with the times measured at DSS 13 (code 0 and 4) and with those unaffected from DSS 14.

Timer 1 was replaced at DSS 13 on 1 April 1976 by a programmable data collector/timer designed by S. S. Brokl (Ref. 8) and programmed by K. I. Moyd. This timer is labeled timer 3, and pertains to configuration code 4.

Occasionally a non-standard value is used for $\Delta f_{\ell}$ in the post-detection filtering. If a correction is applied, the configuration code is 12, corresponding to a correction to code 0 for dates prior to 1970 and to code 5 after 1976. (None occur in the intervening years.)

During the first half of 1979, the SDS 930 computer was phased out of service and removed in June 1979. This created the need to transmit IF signals over the microwave communication links to DSS 14 for data recording. The required 12 MHz bandwidth was obtained from the 6 MHz bandwidth of the link by folding the IF spectrum about the midpoint during base-banding. This technique was also used in obtaining signals from DSS 12. The configuration codes 15 and 16, then, indicate the recording at DSS 14 of signals from DSS 13 and DSS 12, respectively.

The most recent configuration for collecting pulsar data requires the use of the telemetry processor assembly (TPA) found in all DSN stations except DSS 13. The scheme was constructed by J. and M. Urech at DSS 62. Many of the hardware functions of Figure 2 are duplicated by their software. The data output is still in the form of 5000-word records on magnetic tape. The configuration code of this scheme for each station is listed in Table 2.

C. EFFECTS OF RECEIVER PARAMETERS ON THE ARRIVAL TIME

Pulsar signals are dispersive since the interstellar plasma introduces a frequency-dependent group velocity. A broadband pulse, covering the radio spectrum from 30 MHz to 10 GHz, will arrive at the receiving antenna and sweep through the receiver passband at a rate given by

$$\frac{B}{\Delta t} = KF^3/DM \text{ (MHz/sec)} \tag{1}$$

where the bandwidth B is in MHz, the observing frequency F is in MHz, $\Delta t$ is in seconds, DM is the dispersion measure in parsecs (pc) $cm^{-3}$, and $K = 1.205043 \times 10^{-4}$. Let Eq. (1) define the amount of smear $\Delta t$ in the received pulse shape when all the other parameters are known. At F = 2388 MHz, a dispersion measure of 10 pc $cm^{-3}$ causes the pulse to smear 75 μsec when the receiver passband is 12-MHz wide. The smear is 750 μsec when the dispersion measure is 100.

Computed values of smear are presented in Table 4. As long as the bandpass parameters remain fixed over the years, the dispersive effect should not affect the measured arrival times. However, changes in a filter element or the slight alteration in the tuning of the maser amplifier will change the <u>frequency</u> centroid of the passband. This, in turn, will change the <u>time</u> centroid of the detected pulse. The magnitude of this effect must be determined experimentally and has not been done. The effect is expected to be small since it is not the limits of the passband that change, but only the shape.

The response of the post-detection filter is chosen such that the integration time $\tau$ is close to the time interval $P_a/5000$. In the case of these simple RC filters, $\tau = 2RC$ (Ref. 5), where R and C are the filter resistance and capacitance, respectively. Considerable care is exercised in using the appropriate filter combination for each pulsar throughout the observations. Use of non-standard values of $\tau$ could cause up to 200 μsec of time shift in the arrival time. The values are listed in Table 4. Note that the change from pre-10 Jan. 1974 (Code 0) to post-10 Jan. 1974 (Code 0) is principally a change in the post-detection filters, and much care was taken to duplicate the previous values of $\tau$ in the new filters.

A quantitative measure of the system performance is given by the ratio of $\sigma$, the root-mean-square (rms) value of the noise fluctuations about the mean, divided by $\zeta$, the mean. Letting N represent the number of pulses superimposed,

$$\frac{\sigma}{\zeta} = \frac{1}{\sqrt{N\tau B}}$$

Table 4. Pulse Smearing Due to Dispersion and Post-Detection Filtering

| Pulsar | Dispersion Measure* (pc $cm^{-3}$) | Smear for B = 12 MHz (μsec) | Integration Time (μsec) |
|---|---|---|---|
| PSR 0031-07 | 10.89 | 79 | 200 |
| 0329+54 | 26.776 | 195 | 50 |
| 0355+54 | 57.03 | 416 | 50 |
| 0525+21 | 50.955 | 372 | 400 |
| 0628-28 | 34.36 | 251 | 200 |
| 0736-40 | 161.0 | 1174 | 100 |
| 0823+26 | 19.4634 | 142 | 400 |
| 0833-45 | 69.08 | 504 | 50 |
| 0950+08 | 2.969 | 22 | 50 |
| 1133+16 | 4.8479 | 35 | 50 |
| 1237+25 | 9.296 | 68 | 200 |
| 1604-00 | 10.72 | 78 | 100 |
| 1642-03 | 35.71 | 261 | 100 |
| 1706-16 | 24.88 | 182 | 150 |
| 1749-28 | 50.88 | 371 | 400 |
| 1818-04 | 84.38 | 616 | 150 |
| 1911-04 | 89.43 | 653 | 150 |
| 1929+10 | 3.176 | 23 | 50 |
| 1933+16 | 158.53 | 1157 | 50 |
| 2016+28 | 14.176 | 103 | 50 |
| 2021+51 | 22.580 | 165 | 100 |
| 2045-16 | 11.51 | 84 | 200 |
| 2111+46 | 141.50 | 1033 | 200 |
| 2217+47 | 43.54 | 318 | 100 |

*Values From Ref. 22

One expects for $N = 500$, $\tau = 50$ μsec and $B = 12$ MHz, that $\sigma/\zeta \sim 0.0018$. Throughout the years of data collection this parameter has varied between 0.0013 and 0.0025, corresponding to 42 μsec $< \tau <$ 59 μsec. Hence, the values of integration time listed in Table 2 were stable to within 16 percent of the tabulated value.

## SECTION III

## EDITING AND COLLATING

### A. EDITING THE DATA

Successfully measuring the time-of-arrival of a pulse near a given epoch does not ensure that the result is free of biases. The editing process involves detecting the biases, correcting the measurement if the reason for the bias is known, or omitting the measurement if the reason for the bias is known but does not allow correction. A good example of a correctable situation is the use of a receiver frequency other than the 2388 MHz frequency used in most of the measurements.

A preliminary model (position and pulse period) is devised for each pulsar. These models are used in a computer program of adequate accuracy to predict pulse arrival times at the barycenter of the solar system. A barycentric ephemeris of the Earth is used to refer the measured arrival times to the barycenter and a residual (measured minus predicted) arrival time is computed. The occurrence of a residual that is large compared to the average fluctuation is cause for further investigation.

Several properties of the pulsar or the system are directly responsible for the need to correct or omit the arrival time measurement. They are:

(1) Scintillations

Interstellar clouds of ionized hydrogen impose variations on the received pulse power. The time scale of the fluctuations is on the order of tens of minutes. If the pulsar is far enough away, and several are, large fluctuations in the pulse power force the signal down into the receiver noise for many minutes, causing a spurious estimate of the pulse arrival time.

(2) Start Times

The early timing box divides the incoming 1-sec pulse by 10 (see Fig. 4), allowing the counting to be started at well-defined 10-sec intervals. It is imperative that the counter status register be synchronized with the station clock, modulo 10 seconds; i.e., on the even 10-second mark, the counter should read 0. Occasionally synchronization is lost. In these cases it is easy to deduce how many integral seconds (never more than 10) the start time has to be retarded or advanced to obtain the true start time.

(3) Receiver Frequency

Dispersion caused by the interstellar plasma causes the arrival time to be a function of observing frequency. Using a non-standard receiver frequency produces a correctable error (see Section VI, F).

(4) Post-Detection Filter

Occasionally a non-standard filter width was used, resulting in unusual time delay through the filter. A correction is readily applied.

During the summer months of 1969 a bad detector connection caused unusually large (~1 ms) time delays. The corrections for this effect were derived by computing the autocorrelation function of the system noise, the width of which then gave the effective time constant of the filter. Both situations are labeled as system code 12 (see Section II, A).

(5) Miscellaneous

In a very few cases the reasons for a large residual are unknown. Common experimental situations in such cases are receiver tuning problems, repeated power failures, and radio frequency interference (RFI). The measurement results are usually omitted.

B. COLLATING THE DATA

A data tape produced at Goldstone contains data files corresponding to the pulsars observed during a particular observing session. This format is inconvenient for producing average pulse profiles. (These profiles, discussed in Section IV, are a necessary part of optimally estimating the pulse arrival time). Therefore, the early data files of a particular pulsar were gathered onto one or more magnetic tapes in the order they were collected at Goldstone. Preliminary editing took place during this process, to delete obviously faulty data. The main cause for omission at this stage is RFI. These data were used to compute the mean pulse profile presented in Section IV.

Data collected after August of 1972 is not collated according to pulsar. Data files are merely written onto magnetic tapes in the order they were collected without regard to the particular pulsar. The files were condensed by editing the data and filling each tape completely. Estimates of arrival times are obtained after each tape is filled (every 2 to 3 months).

## SECTION IV

## PULSE-SHAPE TEMPLATES

In the presence of white noise the maximum signal-to-noise (S/N) ratio for the output of a particular filter can be obtained when the filter response has the same form as the input signal (a matched filter). The required matched filter is realized by cross correlating a received pulse with an estimate of the noise-free shape of the pulse. The estimates of the noise-free pulse shapes are obtained by superimposing many thousands of pulses to average down the effects of noise. The result is referred to herein as a template.

The proper registration or alignment of the pulses needs to be obtained to build a template with a minimum of smearing. Two passes, each described below, are used to optimize the registration. Correlation with a triangular function is first performed to obtain first-order estimates of pulse position within the data records. The template position in the data array corresponding to the maximum cross correlation coefficient is defined to be the pulse position. The numbers in each data record are then shifted circularly by the amount required for proper registration with all the other data records. Adding all the records produces a preliminary template. This template is cross-correlated with the original data to provide new estimates of pulse positions within the data arrays. The second result of the addition of all the properly registered data is taken as the correct average pulse shape. Finally, the central 4096 words of the 5000 word array are used to form the template. See Section V regarding the choice of the 4096 words.

A. CORRELATION WITH A TRIANGLE

In the early analyses of pulsar data (Ref. 9), the data were cross correlated with a triangular function closely matched in width to the pulsar signal. The pulses resemble the triangular function so the correlation function provides an adequate estimate of the pulse position within the data array.

The shape of the triangular function lends itself to a particularly fast algorithm for computing the cross correlation coefficients. Let the data record be presented by $f_n$, $1 \leq n \leq 5000$. Then correlate with the function

$$T_r(n, n_0, W) = \begin{cases} 1 - \dfrac{|n-n_0|}{W} & ; \dfrac{|n-n_0|}{W} \leq 1 \\ 0 & ; \text{otherwise} \end{cases} \quad (2)$$

W is the half-width of the base of the triangle and $n_0$ is the position of the peak in the data array. This function is shown in Fig. 5 for $n_0$ = W, W+1, and W+2. Inspecting Fig. 5, the correlation coefficients $C_0$ and $C_1$ can be written as

$$C_0 = \sum_{n=1}^{2N-1} T_r(n,W,W)f_n = f_W + \sum_{n=1}^{W-1} \frac{n}{w} f_n + \sum_{n=W+1}^{2W-1} \frac{2W-n}{W} f_n$$

and

$$C_1 = \sum_{n=2}^{2N} T_r(n,W+1,W)\, f_n = f_{W+1} + \sum_{n=2}^{W} \frac{n-1}{W} f_n + \sum_{n=W+2}^{2W} \frac{2W+1-n}{W} f_n$$

The difference between the coefficients becomes

$$C_1 - C_0 = -\frac{1}{W} \sum_{n+1}^{W} (f_n - f_{W+n}) \quad (3)$$

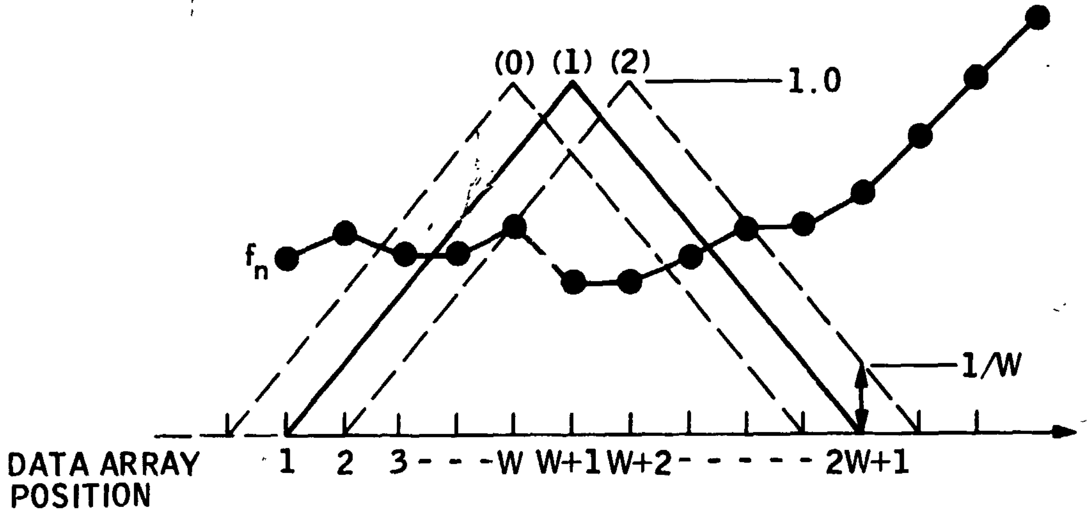


Figure 5. Three Triangular Functions Overlying a Data Array

This is the first quantity computed.

In a similar manner the difference between coefficients $C_2$ and $C_1$ is

$$C_2 - C_1 = -\frac{1}{W} \sum_{n=2}^{W+1} (f_n - f_{W+n}) \tag{4}$$

This is the second quantity computed, but in the following manner. This new quantity is obtained from Eq. (3) by adding the term

$$\frac{f_1}{W} - \frac{2f_{W+1}}{W} - \frac{f_{2W+1}}{W}$$

In general the new difference in adjacent coefficients is computed from the previous difference by

$$C_\ell - C_{\ell-1} = C_{\ell-1} - C_{\ell-2} + \frac{1}{W} (f_{\ell-1} - 2f_{W+\ell-1} + f_{2W+\ell-1}) \tag{5}$$

The value of $C_\ell$ relative to the coefficient $C_1$ is calculated by accumulating the sums $C_\ell - C_{\ell-1} + C_{\ell-1} - C_{\ell-2}$ from Eq. (4) through the many steps suggested by Eq. (5):

$$C_3 - C_2 + C_2 - C_1 = C_3 - C_1$$

$$C_4 - C_3 + C_3 - C_1 = C_4 - C_1$$

$$\vdots$$

$$C_\ell - C_{\ell-1} + C_{\ell-1} - C_1 = C_\ell - C_1$$

The position of the peak of the triangular function corresponding to the largest value of $C_\ell - C_1$ denotes the position of the pulse in the data array.

B. CORRELATION WITH THE TRUE TEMPLATE

The cross correlation function $C(\tau)$ of two continuous functions is written as

$$c(\tau) = \int p(t)e(t - \tau)\, dt \tag{6}$$

where p(t) is the pulse power as a function of time t, e(t) is the expected pulse shape (the pulse template) and $\tau$ is the displacement in time of the two functions relative to some well-defined reference time. In the discrete case encountered here, the correlation coefficients can be evaluated by directly performing the operation suggested in Eq. (6). However, it is much faster to use Fourier analysis techniques. Direct evaluation of Eq. (6) requires $2.5 \times 10^7$ multiplications, while using the fast Fourier transform (FFT) algorithm requires only about $1.4 \times 10^5$ multiplications.

Consider the Fourier transforms of the functions involved. The transform of the correlation function $c(\tau)$ becomes

$$C(s) = \iint p(t)\ e(t - \tau)\ dt\ e^{-i2\pi s\tau}\ d\tau$$

where s is the transform variable. Interchanging the order of integration,

$$C(s) = \int p(t)\ e^{-i2\pi s\tau} \int e(u)\ e^{i2\pi su}\ du\ d\tau$$

or

$$C(s) = P(s)\ E(-s) \tag{7}$$

where P(s) and E(s) are the transforms of p(t) and e(t), respectively. Hence, the procedure is to calculate E(-s) for each template (calculated only once), P(s) for the data record, and then the complex function C(s). Inverse transformation of C(s) yields $c(\tau)$.

The FFT algorithm is used in a form that takes advantage of the fact that a Fourier transform of a real function is the sum of a real even function and an imaginary odd function. Hence, if the data array is L samples long, only L/2 values need be calculated in the transform. See Ref. 10 for the original work on this form of the algorithm or the detailed discussion of its use by Brigham (Ref. 11). Briefly, the data is placed in an array L samples long, where L is a multiple of 2. Pretending that the array is complex of dimension L/2, an FFT is performed on the complex array. A final step is needed to unscramble the result into (L/2) - 1 complex pairs, one 0-frequency value, and one Nyquist-rate value. Alternatively, putting complex data such as the quantities P(s)E(-s) in this form, the inverse of the above process can be formed. Software to perform the calculations was written for this project by G. A. Morris.

The central 4096 data points of the integrated pulse profiles were selected for the templates since the correlation process involves using the FFT algorithm for $2^{12}$ data points. The correlation is done twice to cover all 5000 data points. The details are presented in Section V. The value of $\tau$ corresponding to the maximum value of $c(\tau)$ denotes the position of the pulse in the data array.

## C. SUBTRACTION OF THE BACKGROUND

Once an estimate of the pulse phase has been made, the pulsed power must be separated from the steady component contributed by the system. Let the signal be represented by a pulse template $U(t - \tau)$ of unity maximum height. The pulse is superimposed on a constant term $N_s$ due to system noise. Associated with $N_s$ are small noise variations $n(t)$ caused by a non-zero post-detection bandwidth. Hence, the total signal $S(t)$ becomes

$$S(t) = gU(t - \tau) + n(t) + N_s \tag{8}$$

where g scales the template to the data. The expected value of n, denoted by $E\{n\}$, is zero. The objective is to minimize the quantity

$$I_1 = \int \left[S(t) - gU(t - \tau) - N_s\right]^2 dt \tag{9}$$

All terms in $I_1$ are constant except the term

$$2g \int S(t)\, U(t - \tau)\, dt$$

which must be maximized to minimize $I_1$. But this is merely the cross correlation performed above.

Estimates of g and $N_s$ are needed to separate the pulse from receiver noise. The estimates should minimize $I_1$:

$$\frac{\partial I_1}{\partial g} = 0 = -\int S(t)\, U(t - \hat{\tau})\, dt + g \int U^2(t - \hat{\tau})\, dt + N_s \int U(t - \hat{\tau})\, dt$$

$$\frac{\partial I_1}{\partial N_s} = 0 = -\int S(t)\,dt + g\int U(t-\hat{\tau})\,dt + N_s\int dt$$

where $\hat{\tau}$ is the estimate of $\tau$ from the correlation procedures. Solving for the estimates $\hat{g}$ and $\hat{N}_s$ of g and $N_s$, respectively.

$$\hat{g} = \left[\int dt \int S(t)\,U(t-\hat{\tau})\,dt - \int S(t)\,dt \int U(t-\hat{\tau})\,dt\right] / D$$

$$\hat{N}_s = \left[\int S(t)\,dt \int U^2(t-\hat{\tau})\,dt - \int S(t)\,U(T-\hat{\tau})\,dt \int U(t-\hat{\tau})\,dt\right] / D \tag{10}$$

where

$$D = \int dt \int U^2(t-\hat{\tau})\,dt - \left[\int U(t-\hat{\tau})\,dt\right]^2$$

Note that only the quantities involving S(t) need to be calculated for each data record. All other terms are calculated once for each template.

The discrete version of Eq. (10) is used in the data reduction. The value $\hat{N}_s$ is subtracted from each data record before adding the record to the evolving template.

D. THE TEMPLATES

Several hundred thousand pulses were superimposed as described above to form the final estimates of the average pulse shapes of 24 pulsars. The results appear in Figures 6 through 29. Part (a) of each figure represents the template used in the data reduction. The abscissa presents time in terms of the pulse period P, while the ordinate is in arbitrary units of power. The vertical marks above and below the main pulse define the time origin. Some templates were smoothed beyond the amount inherent in the receiver. The smoothing was obtained by convolving a sinc(t) function of the appropriate width with the original data. The amount of smoothing noted in the figure caption represents the interval from the peak to the first zero of sinc(t). A quantitative discussion of the choice of smoothing is presented in the next section.

Part (b) of each figure presents the details of the pulse on an expanded time scale. If the data has been smoothed more than in part (a) of the figure, the amount of smoothing is noted. The position of the pulse relative to the vertical marks above and below the main pulse defines, for that pulsar, the "zero phase" condition relative to a given epoch; i.e., to obtain a zero time-of-arrival residual relative to a given epoch, the vertical marks must be coincident with that epoch.

## E. TEMPLATE SMOOTHING

The accuracy with which one can estimate the arrival time of a pulse increases as the random fluctuations in the signal decrease and as the sharpness of the pulse increases. However, attempts to smooth the signal to lower the effects of receiver noise also tend to destroy the sharpness of the pulse. A compromise must then be reached. This is done by estimating the uncertainty in the arrival time measurement when the signal-to-noise ratio is large.

Imagine that having performed the correlation process to measure the arrival time of the pulse, an estimate $\hat{\tau}$ has been obtained. The scaling of the template, $\hat{g}$, and the constant component, $\hat{N}_s$, have also been estimated. Allowing for small errors in the estimates, the model of Eq. (8) can be rewritten as a Taylor expansion:

$$S(\tau) = \hat{g}U(\Delta\tau) + \Delta gU(\Delta\tau) - \hat{g}\Delta\tau U'(\Delta\tau) + \hat{N}_s + \Delta N_s + n(\Delta\tau) \qquad (11)$$

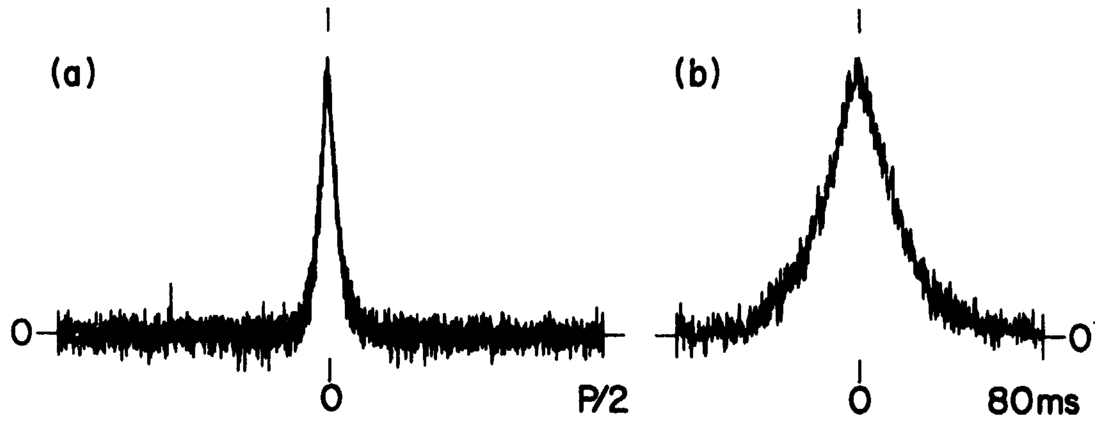


Figure 6. The template of PSR 0031-07: (a) P = 0.943 sec; (b) Expanded time scale

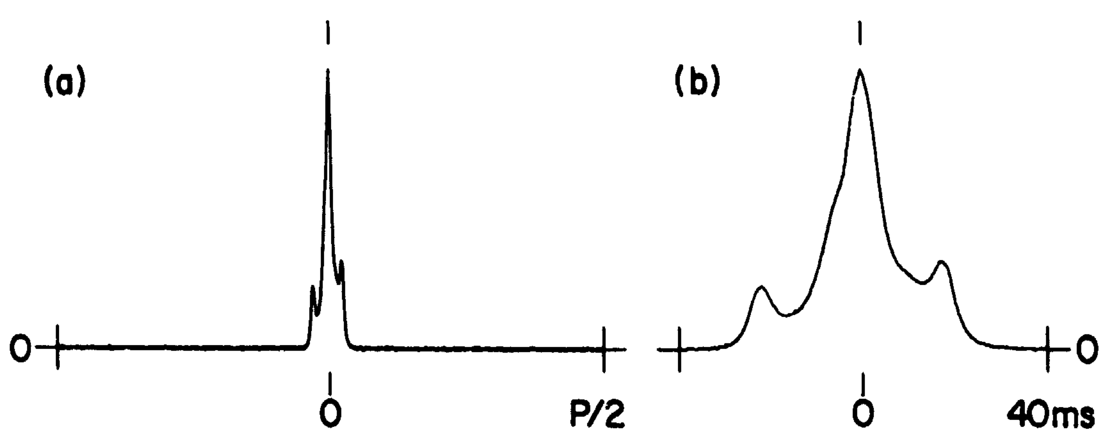


Figure 7. The template of PSR 0329+54: (a) P = 0.715 sec; (b) Expanded time scale

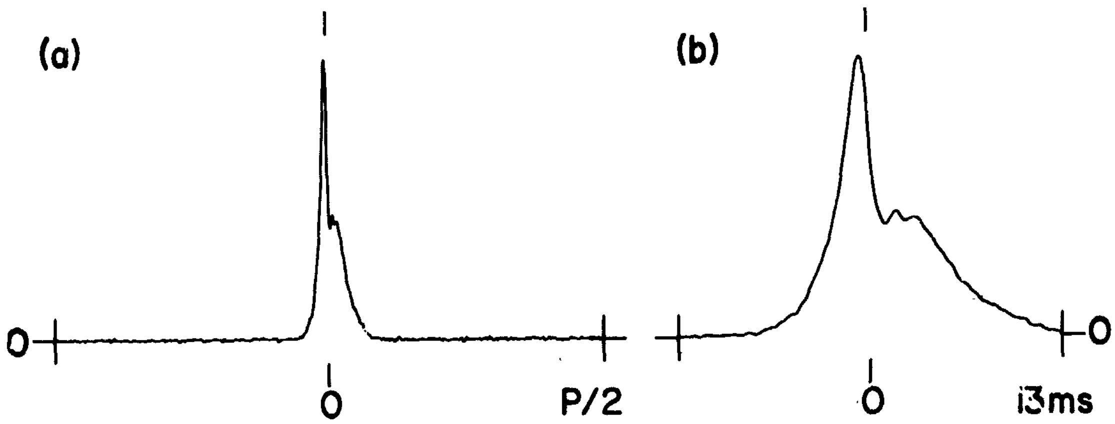


Figure 8. The template of PSR 0355+54: (a) P = 0.156 sec. The pulse has been smoothed by a window 160 μsec wide. (b) Expanded time scale

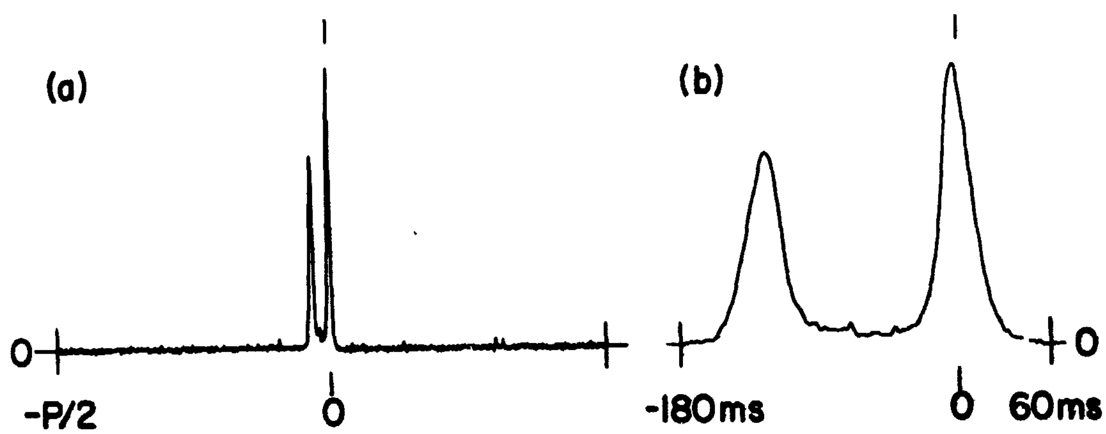


Figure 9. The template of PSR 0525+21. (a) P = 3.745 sec. The pulse has been smoothed by a window 2.2 ms wide. (b) Expanded time scale

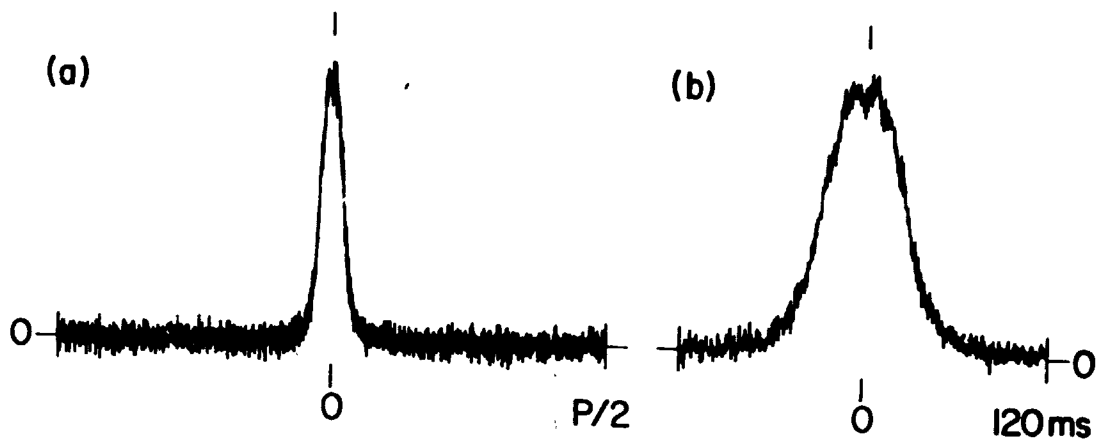


Figure 10. The template of PSR 0628-28: (a) P = 1.244 sec;
(b) Expanded time scale

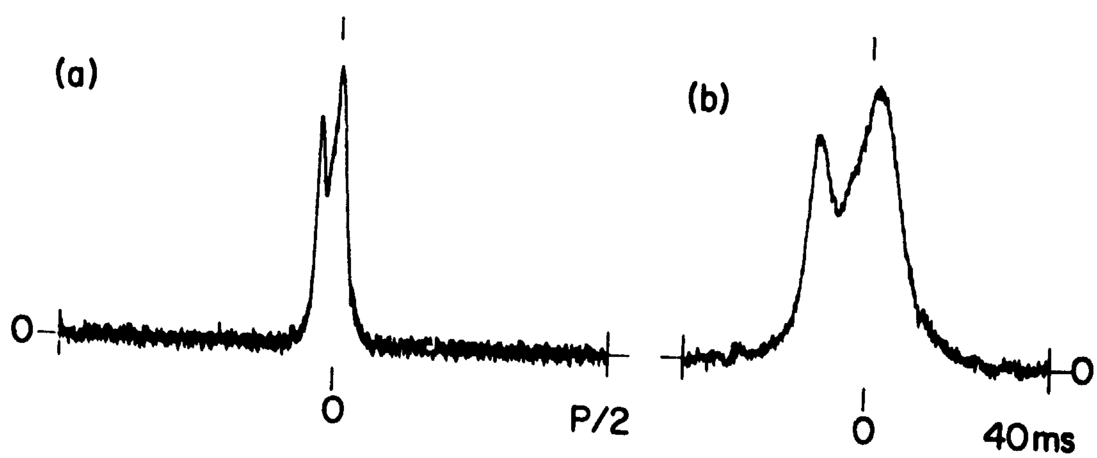


Figure 11. The template of PSR 0736-40: (a) P = 0.374 sec;
(b) Expanded time scale

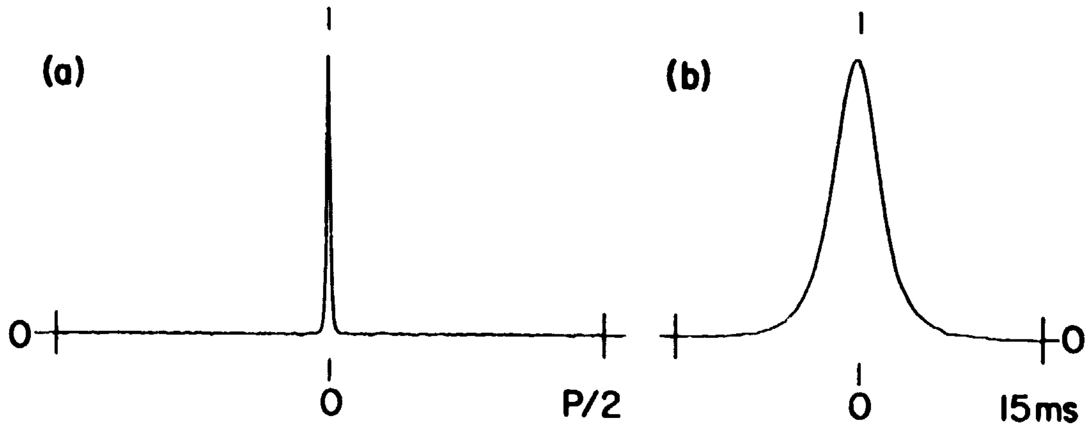


Figure 12. The template of PSR 0823+26: (a) P = 0.531 sec; (b) Expanded time scale

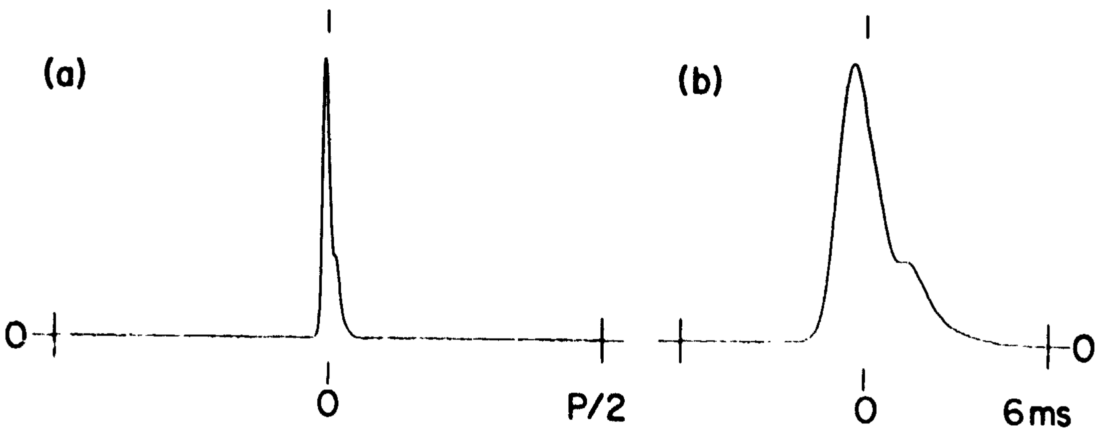


Figure 13. The template of PSR 0833-45: (a) P = 0.089 sec; (b) Expanded time scale

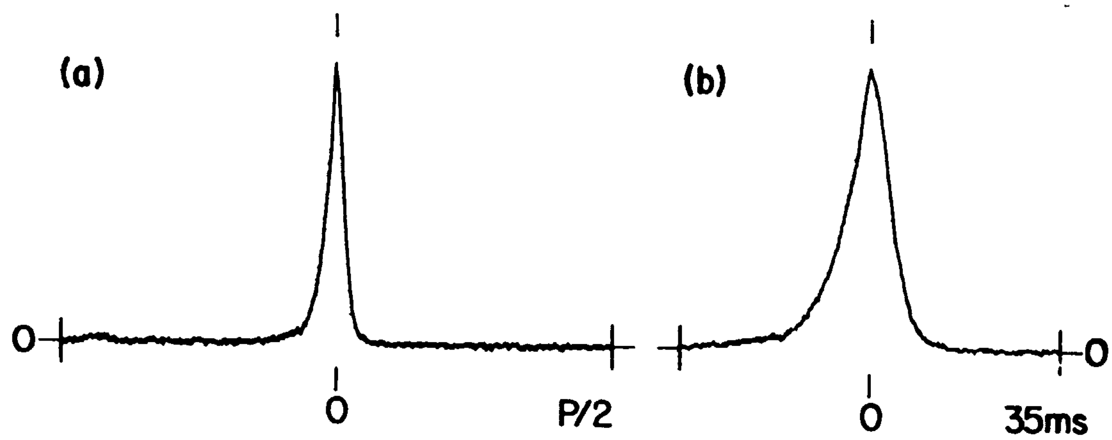


Figure 14. The template of PSR 0950+08: (a) P = 0.253 sec;
(b) Expanded time scale

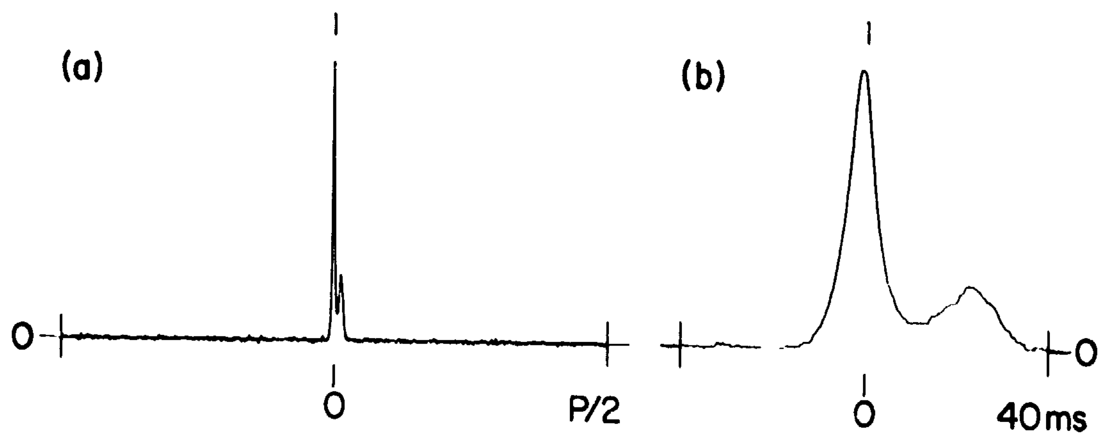


Figure 15. The template of PSR 1133+16: (a) P = 1.188 sec;
(b) Expanded time scale

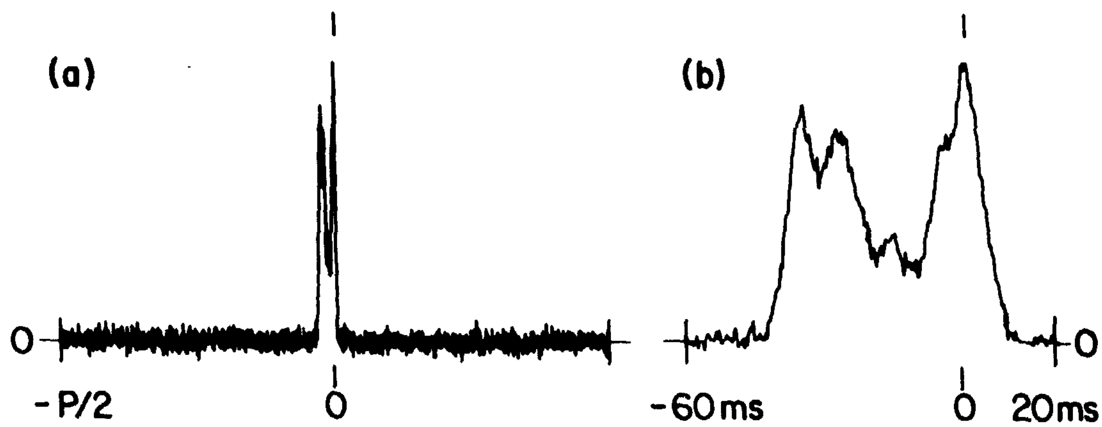


Figure 16. The template of PSR 1237+25: (a) P = 1.382 sec; (b) Expanded time scale

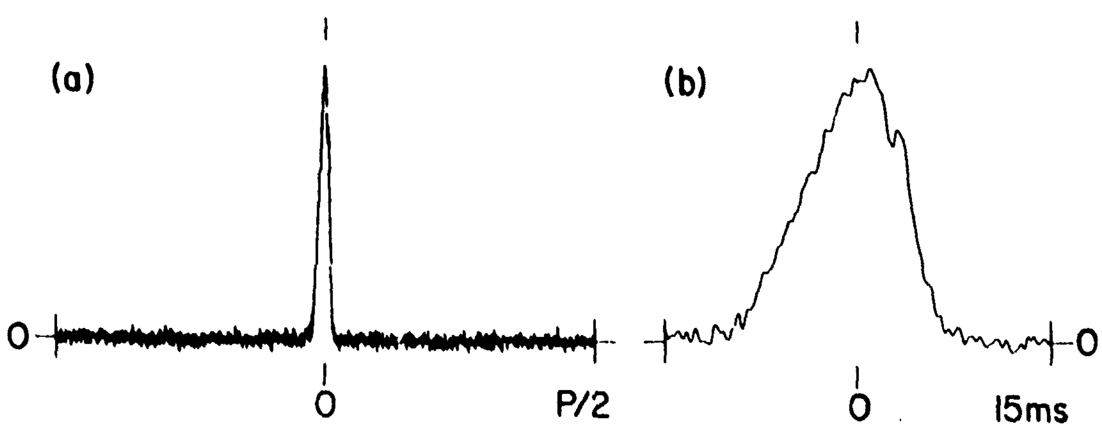


Figure 17. The template of PSR 1604-00: (a) P = 0.422 sec; (b) Expanded time scale

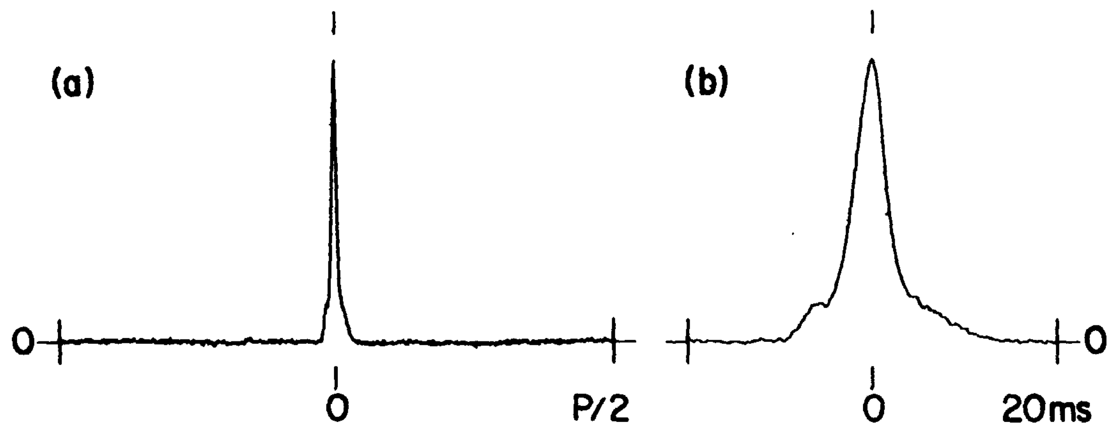


Figure 18. The template of PSR 1642-03: (a) P = 0.388 sec; The data has been smoothed by a window 230 μsec wide. (b) Expanded time scale

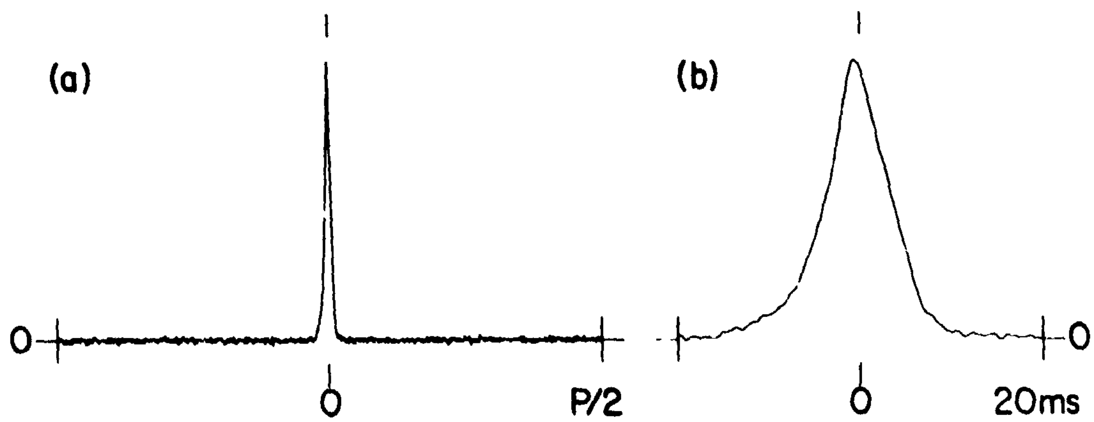


Figure 19. The template of PSR 1706-16: (a) P = 0.653 sec; The data has been smoothed by a window 390 μsec wide. (b) Expanded time scale

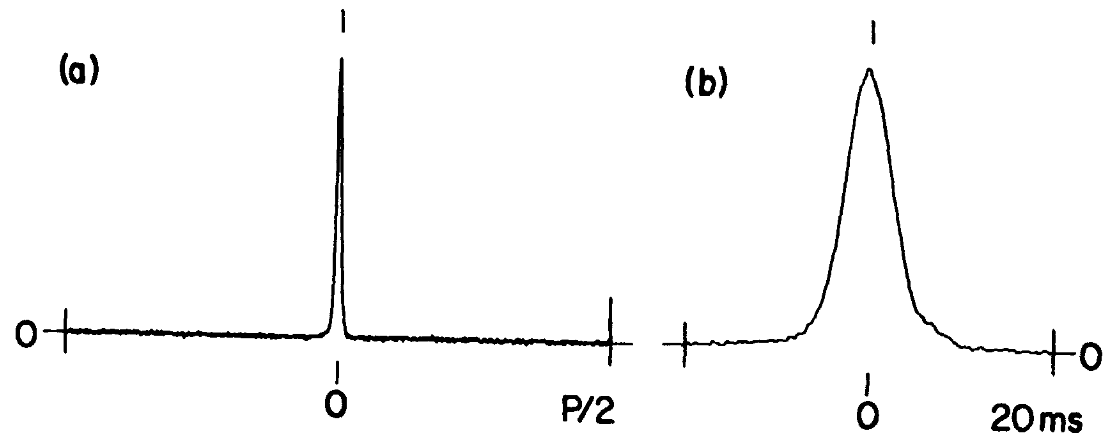


Figure 20. The template of PSR 1749-28: (a) P = 0.563 sec; (b) Expanded time scale

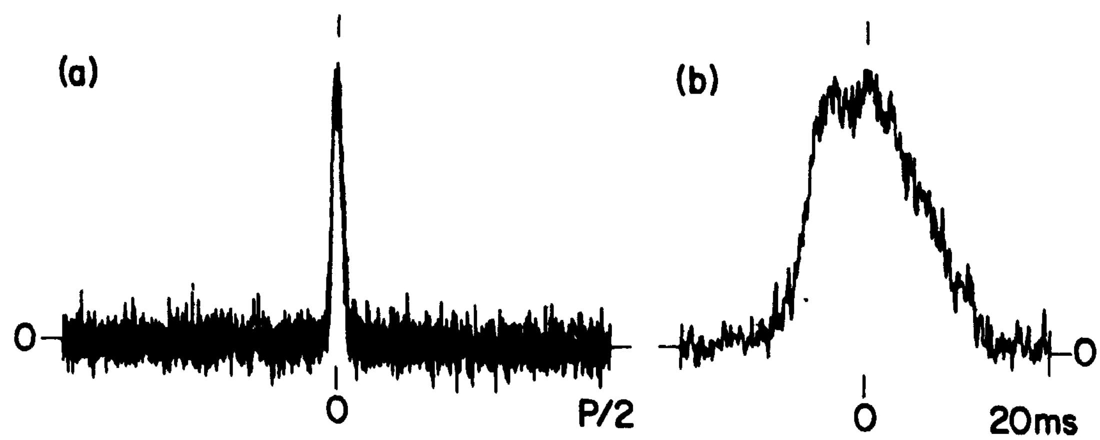


Figure 21. The template of PSR 1818-04: (a) P = 0.598 sec; (b) Expanded time scale

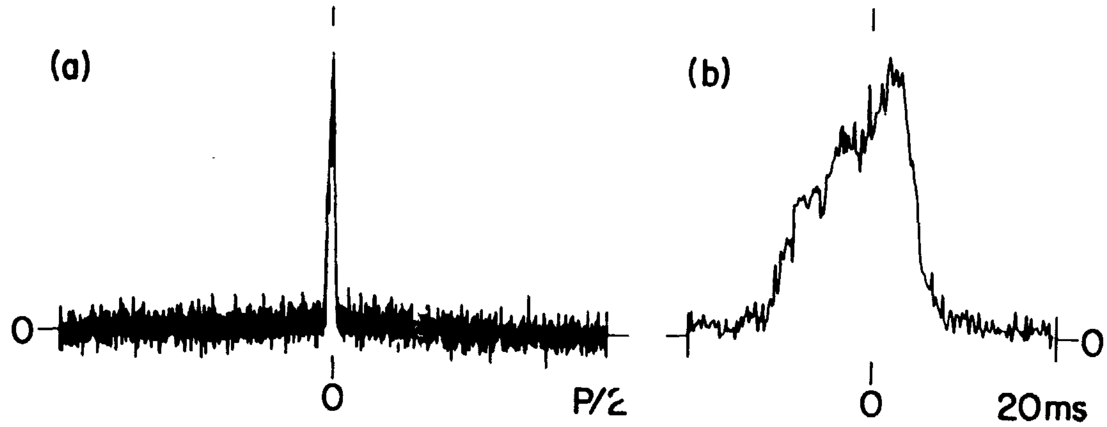


Figure 22. The template of PSR 1911-04: (a) P = 0.826 sec; (b) Expanded time scale

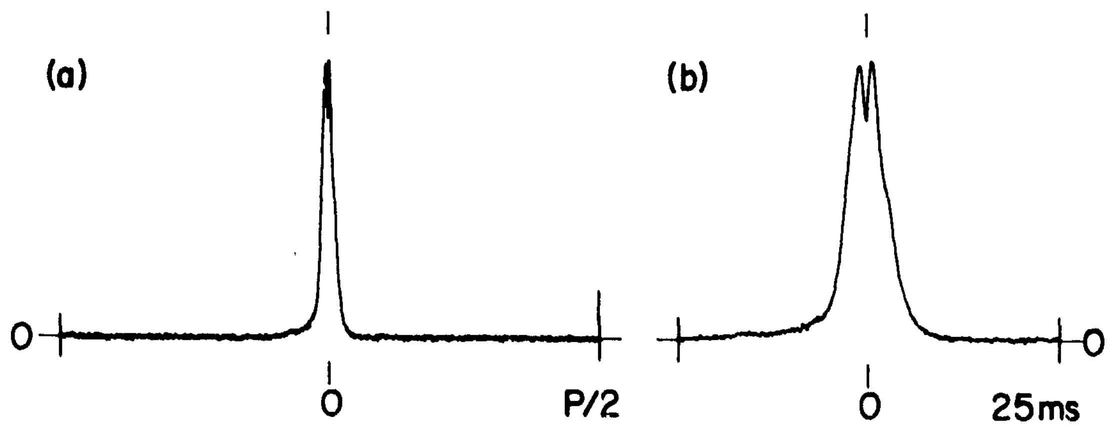


Figure 23. The template of PSR 1929+10: (a) P = 0.227 sec; (b) Expanded time scale

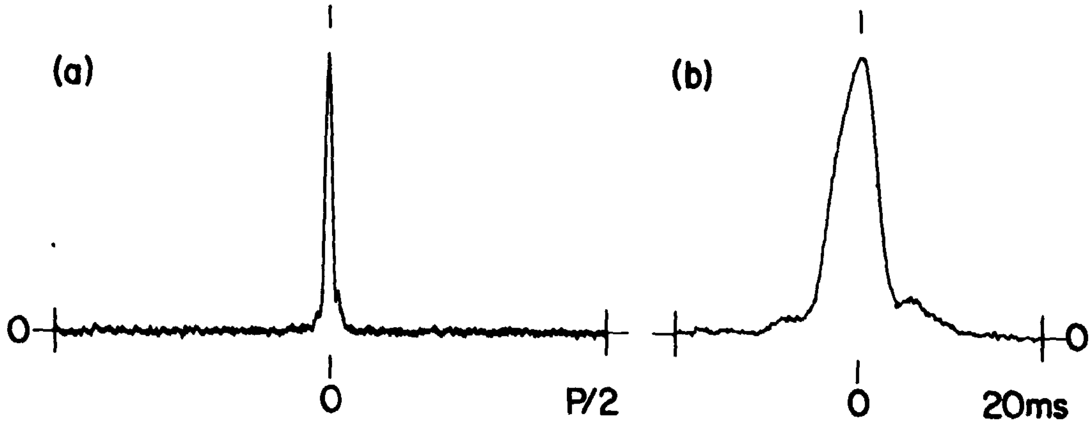


Figure 24. The template of PSR 1933+16: (a) P = 0.359 sec; (b) Expanded time scale

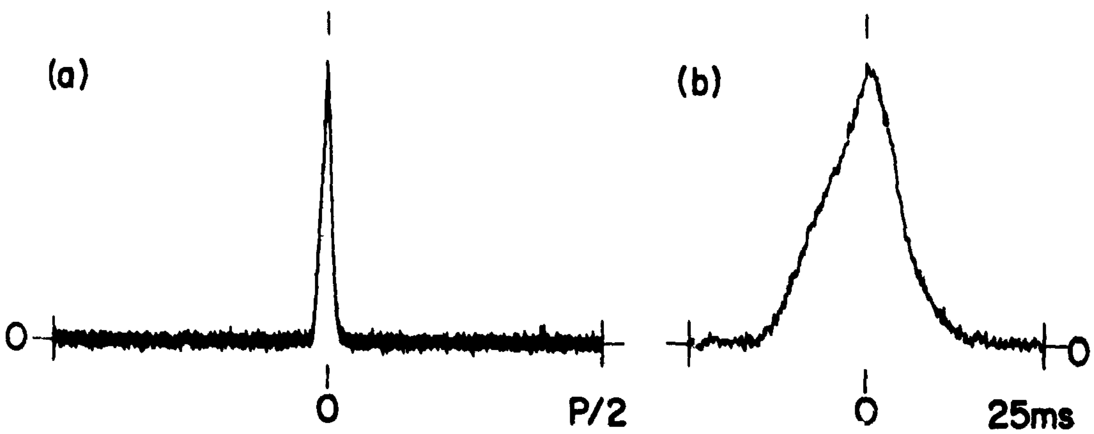


Figure 25. The template of PSR 2016+28: (a) P = 0.559 sec; (b) Expanded time scale

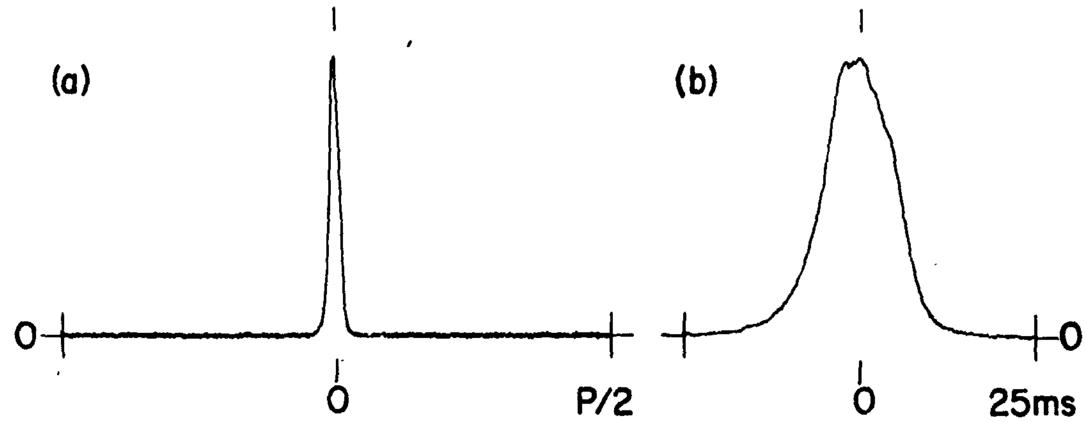


Figure 26. The template of PSR 2021+51: (a) P = 0.529 sec; (b) Expanded time scale

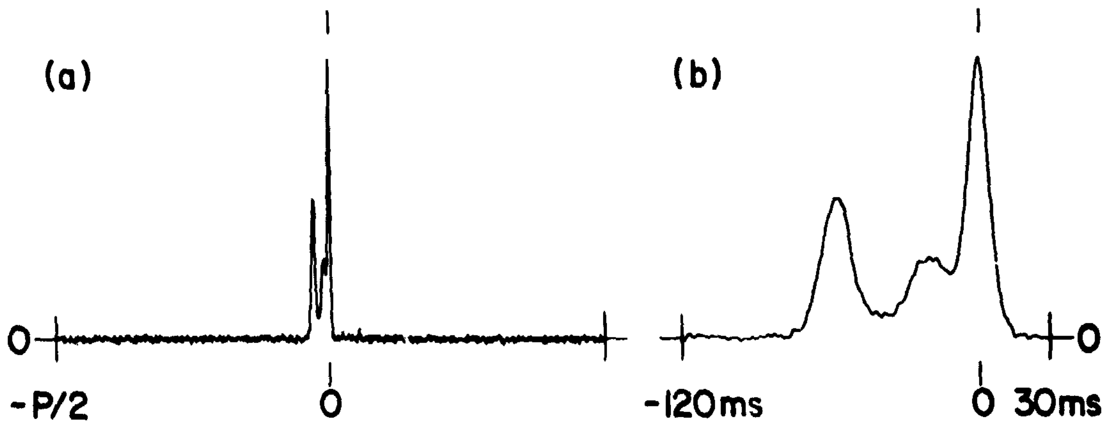


Figure 27. The template of PSR 2045-16: (a) P = 1.96_ sec. The data has been smoothed by a window 1.2 ms wide. (b) Expanded time scale

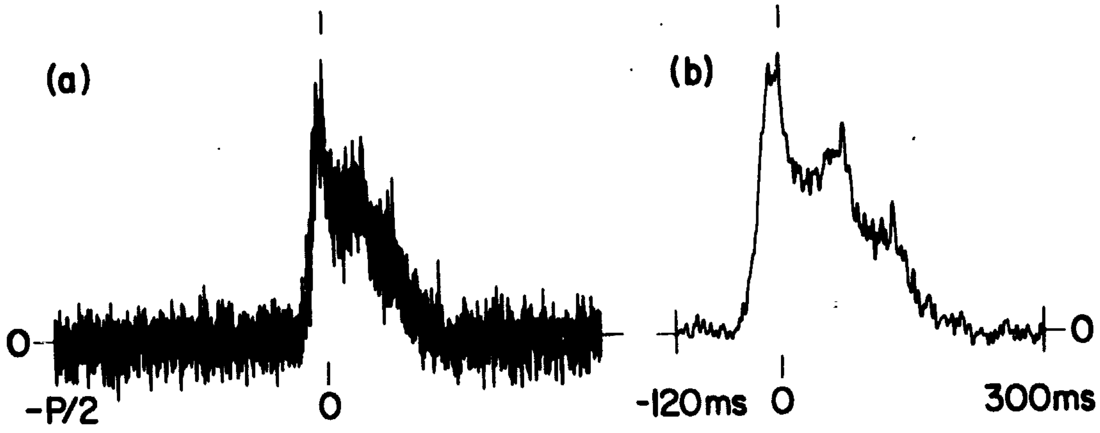


Figure 28. The template of PSR 2111+46: (a) P = 1.015 sec; (b) Expanded time scale, with the data smoothed for display by a window 2.0 ms wide

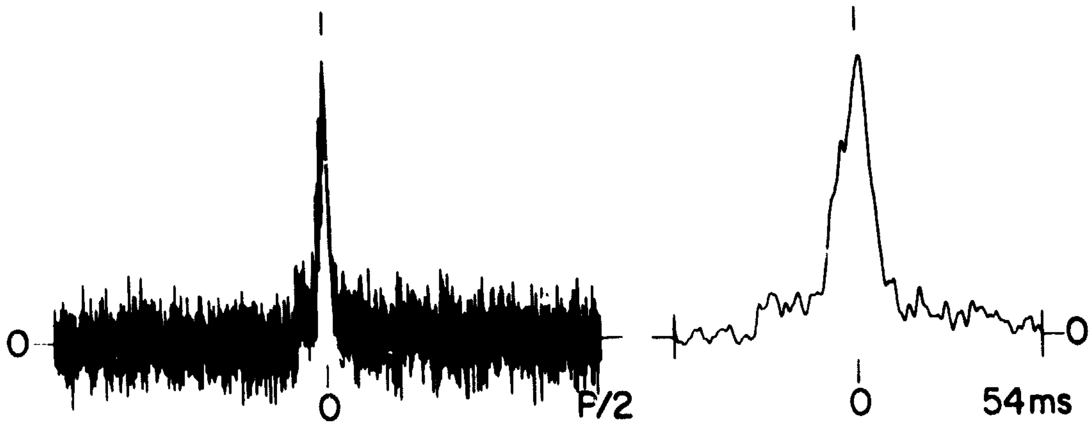


Figure 29. The template of PSR 2217+47: (a) P = 0.538 sec; (b) Expanded time scale, with the data smoothed for display by a window 1 ms wide

where the prime denotes a derivative, and

$$\Delta g = g - \hat{g},\ \Delta N_s = N_s - \hat{N}_s \text{ and } \Delta\tau = \tau - \hat{\tau}$$

Substituting Eq. (11) into Eq. (9) yields the mean square error in using estimates $\hat{g}$, $\hat{N}_s$ and $\hat{\tau}$ instead of the mean values $g$, $N_s$ and $\tau$. Minimize the mean square error with respect to $\Delta\tau$ to obtain

$$\frac{\partial I_1}{\partial \Delta\tau} = 2 \int_0^P \left[\Delta g U(\Delta\tau) - \hat{g}\Delta\tau U'(\Delta\tau) + \Delta N_s + n(\Delta\tau)\right]$$

$$\times \left[\Delta g U'(\Delta\tau) - \hat{g}U'(\Delta\tau) - \hat{g}\Delta\tau U''(\Delta\tau) + n'(\Delta\tau)\right] d\tau = 0$$

where

$U' = dU/dt$, $U'' = d^2U/dt^2$, etc. The integration is over one full pulse period. Collecting terms, we make use of the following facts:

(1) $U(0) = U(P) = 0$

(2) $U'(0) = U'(P) = 0$

(3) $\int n' \, d\tau = n(0) - n(P) \approx 0$

and

(4) $\int n\, n' \, d\tau \approx 0$

Then

$$\Delta\tau \approx \frac{\int U' n \, d\tau}{\hat{g} \int (U')^2 \, d\tau} \tag{12}$$

where terms of the order $\Delta g/\hat{g}$ have been omitted.

Since

$$E\{\Delta\tau\} = \int U' \, E\{n\} d\tau / \hat{g} \int (U')^2 \, d\tau = 0,$$

then

$$\sigma_\tau^2 = E\{\Delta\tau^2\} = \frac{E\left\{\int U'(s)\ n(s)\ ds \cdot \int U'(q)\ n(q)dq\right\}}{\hat{g}^2\left[\int (U')^2\ d\tau\right]^2}$$

or

$$\sigma_\tau^2 = \frac{\iint U'(s)\ U'(q)\ R_n(s-q)\ ds\ dq}{\hat{g}^2\left[\int (U')^2\ d\tau\right]^2}$$

where $R_n(\Delta\tau)$ is the auto-correlation function of the random fluctuation $n(t)$. $R_n(0) = \sigma_n^2$. If $R_n$ always decreases significantly before U' can change significantly, then this result remains independent of the post-detection bandwidth. Measuring the variance of the fluctuations in a region not containing the pulse, we can write

$$\sigma_\tau \approx \frac{\sigma_n / \hat{g}}{\left[\int_0^P (U')^2\ d\tau\right]^{1/2}} \tag{13}$$

The denominator is corrected for contributions to U' from random fluctuations. The expected standard deviation associated with $\hat{\tau}$ is then $\sigma_\tau$.

The expression for $\sigma_\tau$ satisfies our intuition with respect to how well $\tau$ can be measured for a given signal-to-noise ratio ($\hat{g}/\sigma_n$) and a given pulse sharpness (measured by $\int (U')^2\ d\tau$). A test of Eq. (13) was performed which did not rely on intuition. The extremely noise-free template for PSR 0833-45 was used as the basis for producing 100 records of simulated data. A random number generator was used to superimpose uncorrelated fluctuations onto the original template. Equation (13) was used to choose the variance $\sigma_n^2$ given that $\sigma_\tau$ = 5 μsec. The sharpness $\int (U')^2 \, d\tau$ is known from the template, and g = 1 in this case.

Would the correlation method define a random process $\hat{\tau}$ from the 100 simulated data records with the correct standard deviation? It did. The true value of τ was known in this test, and the standard deviation of the estimates $\hat{\tau}$ about the expected value τ was 5.2 μsec.

The templates were smoothed to the resolution where $\sigma_\tau$ stopped decreasing due to a lower $\sigma_n$ and began increasing due to loss in sharpness of the pulse.

F. CENTRAL SPIKES

Occasionally, the pulse strength in some of the weaker pulsars ebbs to the point of invisibility (a S/N ratio of 1 or less), even after an hour of integration. In these data records the template seeks out the stronger, sharper random fluctuations. The resulting estimate of τ represents the position in the data array of one of the larger noise spikes. In superimposing data records to produce a template, a narrow central spike was formed.

The central spike phenomenon was observed in the templates for PSR 1818-04 and PSR 2111+46. The spike was removed by placing in the central nine array locations a random process with a mean computed from the eight neighboring values. The variance was set equal to that of the pulse-free portion of the array.

G. DEFINING THE ZERO-LEVEL

Defining the zero-level of the pulsed radiation is straightforward in the cases where the pulses are narrow and confined to one window. This is not to say that the radiation between the pulses is not in part pulsed and associated with the pulsar. In most cases, however, the emission is featureless. If a portion of the flat interpulse region is also pulsed, measurements of a different nature are required to detect this possible situation. In general, the mean value of the interpulse emission is used to define the zero-level.

In several cases, such as PSR 0950+08, the presence of sharp or broad features requires a careful definition of the interpulse region. In these carefully defined regions the mean value is then taken to be the zero-level of pulsed emission.

## SECTION V

## ESTIMATING THE PULSE ARRIVAL TIME

Each data record on magnetic tape presents an opportunity to measure the arrival time of a received pulse relative to a given epoch. The measurement is completed by correlating the appropriate template (Figures 6 through 29) with data records represented by Figure 1. The correlation process leads to an estimate of the maximum cross-correlation coefficient. However, the coefficients occur only every $P_a/5000$ seconds of delay, so interpolation in the neighborhood of the largest coefficient is required to obtain the best estimate of the delay corresponding to the true maximum of the coefficients. The value of the largest correlation coefficient and an estimate of the random fluctuations due to receiver noise are used to estimate the uncertainty in the time delay.

### A. THE CORRELATION PROCESS

The data records are 5000 words long. Two arrays of 4096 words each are constructed to allow easy use of the FFT algorithm. The two separate results, each 4096 words, are combined to yield one 5000-word array of cross-correlation coefficients.

The template is shifted in position before transformation, as shown in Figure 30. The time within each pulse corresponding to <u>the arrival time of the pulse</u> is, in practice, the time marked "0" in Figures 6 through 29. Each template is shifted circularly until this time occurs in the first word of each array. Hence, the position of the largest correlation coefficient will be the estimate of the arrival time of that particular pulse. In addition, this shift keeps the size of the imaginary component of the transformed template to a minimum.

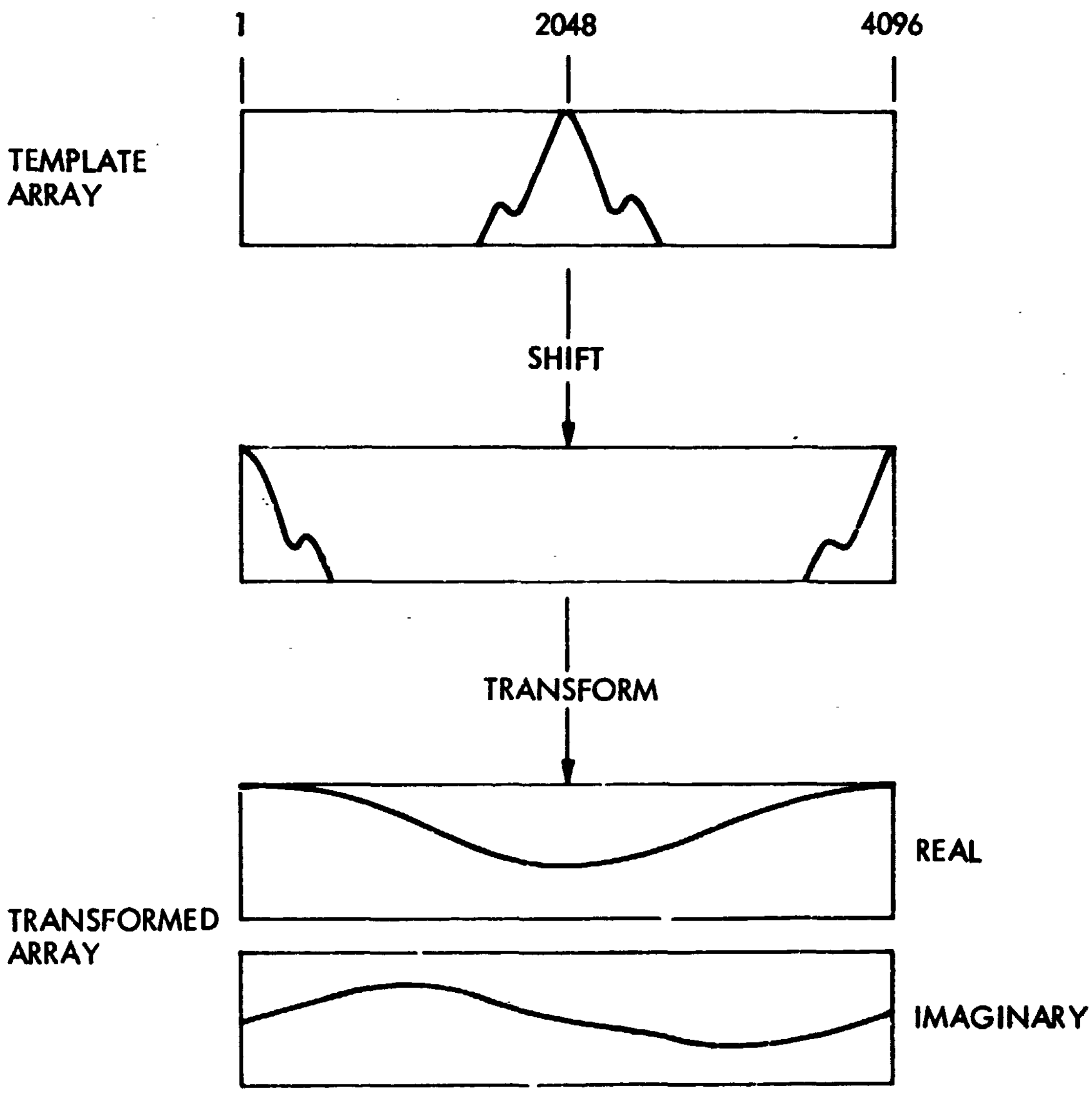


Figure 30. Shifting and Transforming the Template

obtained when no smearing is present represents a bias that can be estimated and removed. The bias is estimated by first calculating the expected arrival time based on the model of the pulsar, and then comparing that with the arrival time expected for a pulsar with a constant period and constant Doppler shift. The mean of the differences is the estimate of the bias.

The expected arrival time $t_k$ of the $k^{th}$ pulse arriving after the starting epoch $t_0$ is given by

$$t_k = t_{bk} + \frac{1}{c}\left[d(t_k) - d(t_0)\right] \tag{15}$$

where $t_{bk}$ is the elapsed time between k pulses at the barycenter of the solar system, d(t) is the distance of the received wavefront from the barycenter, and c is the velocity of light. Expanding the barycentric pulse period P(t) in a Taylor series about $t_0$,

$$P = P_0 + \dot{P}_0(t - t_0) + \ddot{P}_0(t - t_0)^2/2 + 0(\dddot{P}\ t^3)$$

It can then be shown that

$$t_{bk} \approx k\ P_0 + k^2\ P_0\ \dot{P}_0/2 + 0(k^3\ P) \tag{16}$$

The quantity d(t) can be replaced with the scalar product $-\overline{r}_a(t) \cdot \overline{U}_p(t)$, where $\overline{r}_a(t)$ is the position vector of the antenna relative to the barycenter at time t. The unit vector $\overline{U}_p$ is the direction vector of the pulsar as seen from the barycenter. Referring to Figure 34, note that $|\overline{r}_a| = a \sim 1$ AU, and R/a >> 1. Using the facts that

$$Y = -a \cos\theta - d$$

$$2(R-d)Y = X^2 + Y^2$$

and

$$X^2 + Y^2 = Z^2 = d^2 + a^2 + 2ad \cos\theta,$$

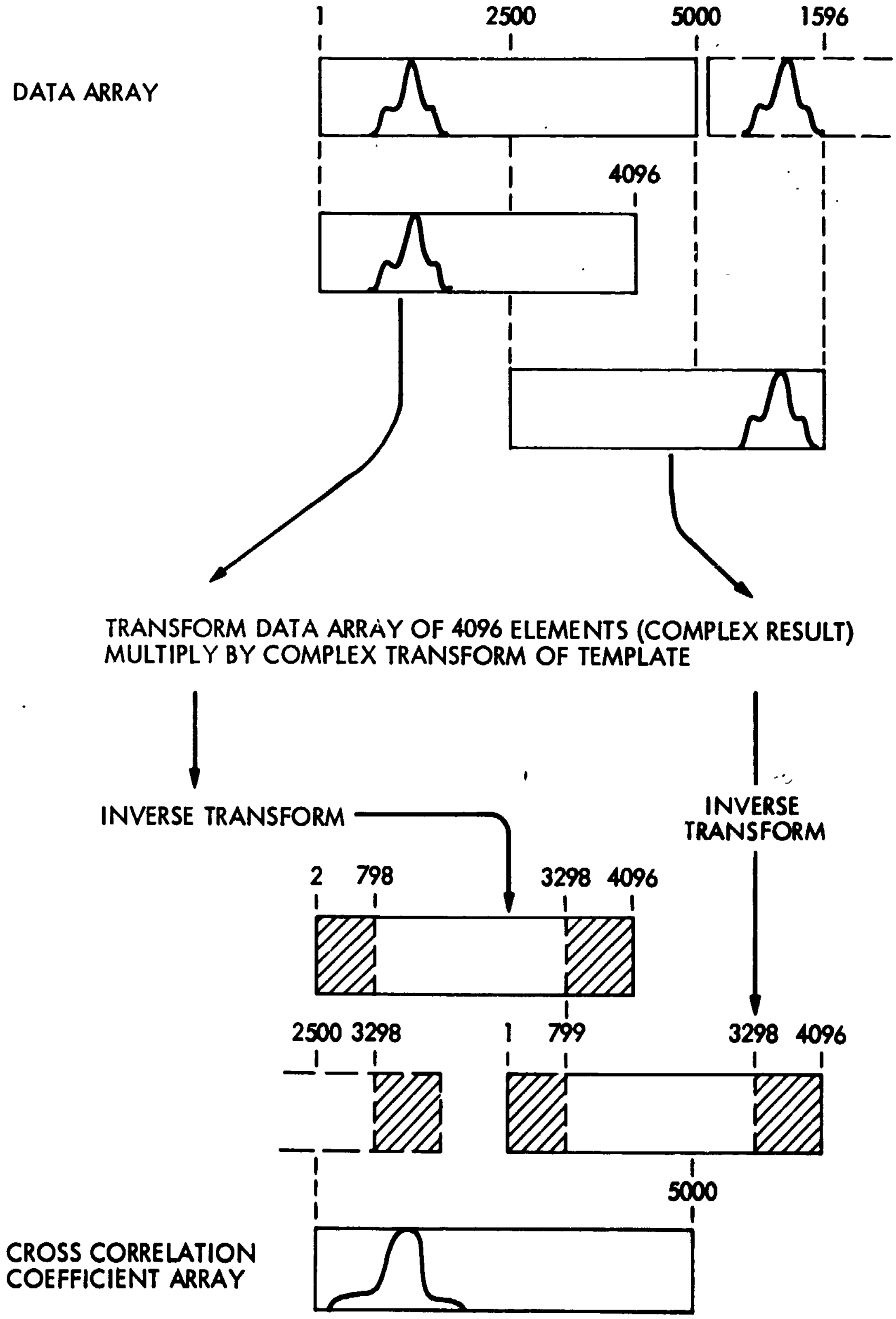


Figure 31. Computing the Cross Correlation Coefficients

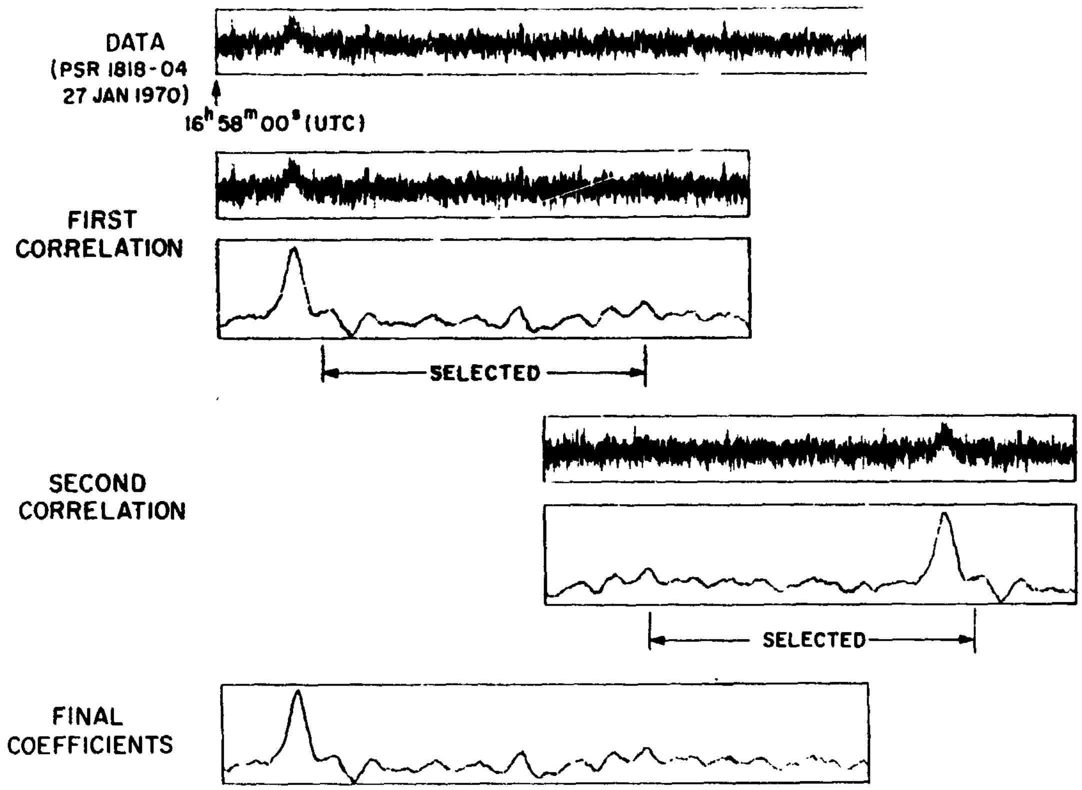


Figure 32. An Example of the Cross Correlation Process; PSR 1818-04 on 27 Jan. 1970 at $16^h\ 58^m\ 00^s$ UT

## B. ESTIMATING THE DELAY

The correlation coefficients are examined to determine the position in the array of the largest coefficient. In the cases of PSR 0355+54 and PSR 0833-45, two and three pulses, respectively, occur per data record. In these cases two or three positions are determined, each separated by a pulse period, and averaged together at the end of the estimation process.

Subsequent refinement of the estimate of the pulse position is obtained through interpolation. Interpolation is obtained by fitting, in a least-square sense, a fourth-order polynomial to M coefficients either side of the largest coefficient. At position $x_1$ (measured relative to the position of the largest coefficient) in the array of correlation coefficients, a predicted value of $C_i = \sum_{\ell=0}^{4} a_\ell \, x_i^\ell$ is obtained. Note that $x_{i+1} - x_i = 1$. We have for the 2M + 1 coefficients involved,

$$C_{-M} = a_0 + a_1 x_{-M} + \dots a_4 x_{-M}^4$$

$$\vdots$$

$$C_0 = a_0$$

$$C_1 = a_0 + a_1 x_1 + \dots a_4 x_1^4$$

$$\vdots$$

$$C_M = a_0 + a_1 x_M + \dots a_4 x_M^4$$

The polynomial coefficients $a_j$ need to be determined. Denoting the measured coefficient by $\hat{C}_i$, we want to minimize the quantity

$$S = \sum_{i=-M}^{M} (\hat{C}_i - C_i)^2 = \sum_i \left[ \hat{C}_i - \sum_{\ell=0}^{4} a_\ell x_i^\ell \right]^2$$

Requiring $\frac{\partial S}{\partial a_\ell} = 0$ for $\ell = 0$ to 4, we find the set of equations

$$\ell = 0; \sum_{i=-M}^{M} \hat{C}_i = a_0 + a_1 \sum_i x_i + a_2 \sum_i x_i^2 + a_3 \sum_i x_i^3 + a_4 \sum_i x_i^4$$

$$\ell = 1; \sum_{i=-M}^{M} \hat{C}_i x_i = a_0 \sum_i x_i + a_1 \sum_i x_i^2 + \dots a_4 \sum_i x_i^5 \tag{14}$$

$$\vdots$$

$$\ell = 4; \sum_{i=-M}^{M} \hat{C}_i x_i^4 = a_0 \sum_i x_i^4 + a_1 \sum_i x_i^5 + \dots + a_4 \sum_i x_i^8$$

Since the $x_i$ occur at uniform intervals, the sums of odd powers of $x_i$ are zero, and the sums of even powers of $x_i$ are precomputed for each pulsar. The size of M is chosen separately for each pulsar. Within the range $x_{-M} < x_i < x_M$, the fourth-order polynomial provides a good fit to the correlation coefficients obtained when the template is correlated with itself.

The system of equations in Eq. (14) is solved for the polynomial coefficients $a_\ell$. The curvature of the resulting polynomial is computed. A positive second derivative indicates a distortion due to a low signal-to-noise ratio, and the interpolation is not attempted. Otherwise, the position $x_p$ at which the polynomial peaked is determined. Then, stepping in intervals of 0.01 between $x_p$-1 and $x_p$+1, the refined estimate $x_d$ of where the polynomial reaches its peak is determined.

The arrival time $t_a$ of the first pulse occuring after the start time $t_s$ is readily calculated. The separation between data array elements is $P_a$/5000 seconds. Hence, $t_a = t_s + x_d\ P_a/5000$.

The interpolation performed near the peak coefficient in Figure 32 is presented in Figure 33. The measured values of the cross-correlation coefficients (solid circles) are displayed versus the corresponding array location, which is proportional to time delay. The solid curve is the polynomial resulting from the least-squares fit. The peak of the polynomial is near x = 589.0. The region near this value of x is enclosed by the broken box, and reproduced on a finer scale in the inset. Progressing from x = 589 to x = 590 in steps of 0.01, the peak, denoted by the vertical arrow, is found at $x_d$ = 589.79.

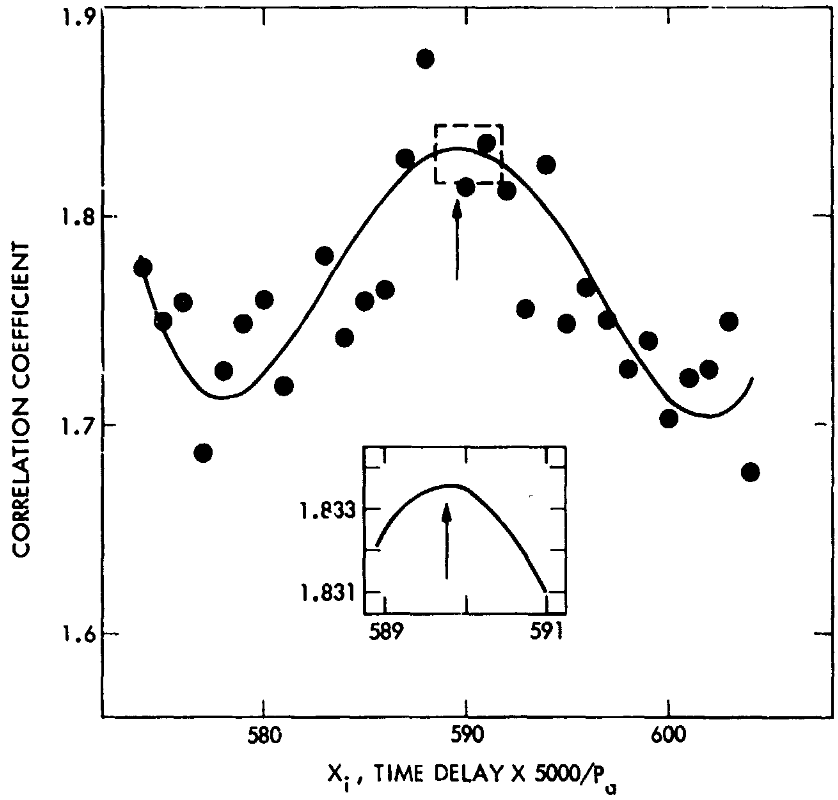


Figure 33. Correlation Coefficients Versus Time Delay Near the Peak Shown in Figure 32

C. ADJUSTMENTS

If the template has been shifted due to a large asymetry about the zero-phase position, the effect of that shift is removed at this point in the data reduction. If two or three estimates of $x_d$ were made, they are averaged together at this point.

D. UNCERTAINTY IN THE ARRIVAL TIME

Each estimate of the arrival time $\hat{\tau}$ is accompanied by an estimate of the uncertainty $\sigma_\tau$. A modification of Eq. (13) is used. The scale factor $\hat{g}$ and the baseline level $\hat{N}_s$ are first estimated using Eq. (10). Quantities dependent on the template $U(\tau)$ only, having been computed earlier in the template generating process, are on magnetic tape with the template itself. Note that the quantity $\int S(t)U(t - \hat{\tau})\, dt$ is merely the maximum correlation coefficient. The root-mean-square (rms) noise level $\sigma_n$ includes a contribution by the template. The denominator of Eq. (13) is another quantity computed earlier.

## SECTION VI

## GEOCENTRIC ARRIVAL TIMES

Now that the arrival time of the pulse has been measured relative to an epoch defined by a particular clock, it is time to consider referring these station arrival times to the geocenter. There are several corrections which must be applied to the measured arrival time before useful geocentric results are obtained: (a) A bias in the arrival time, caused by the smearing of the pulse during superposition, must be estimated and removed; (b) the geometric correction, changing the spatial reference from the antenna to the geocenter, must be applied; (c) an extra delay must be removed which is caused by using frequencies lower than 2388 MHz; (d) a small annual effect caused by the interaction of the Doppler and dispersion phenomena must be removed; (e) the clock epochs used in the measurements must be expressed as Coordinated Universal Time (UTC) epochs; (f) UTC epochs must then be expressed as ephemeris time (ET) epochs. The result is then the arrival time that would have been obtained had the measurement been performed at the geocenter using a clock running on ephemeris time.

### A. CORRECTION FOR PULSE SMEARING

A small amount of smearing is inevitable as the received pulses are superimposed. The Doppler shift caused by Earth's rotation and orbital motion changes over the interval of integration. Also, differences can exist between the actual pulse period and the assumed period. The result is a slow drift in the pulse phase relative to the starting epoch, causing the centroid of the integrated signal to drift forward or backward in time as pulses are superimposed. The difference between the phase of the centroid of the superimposed pulses and the phase obtained when no smearing is present represents a bias that can be estimated and removed. The bias is estimated by first calculating the expected arrival time based on the model of the pulsar, and then comparing that with the arrival time expected for a pulsar with a constant period and constant Doppler shift. The mean of the differences is the estimate of the bias.

The expected arrival time $t_k$ of the $k^{th}$ pulse arriving after the starting epoch $t_0$ is given by

$$t_k = t_{bk} + \frac{1}{c}\left[d(t_k) - d(t_0)\right] \tag{15}$$

where $t_{bk}$ is the elapsed time between k pulses at the barycenter of the solar system, d(t) is the distance of the received wavefront from the barycenter, and c is the velocity of light. Expanding the barycentric pulse period P(t) in a Taylor series about $t_0$,

$$P = P_0 + \dot{P}_0(t - t_0) + \ddot{P}_0(t - t_0)^2/2 + 0(\dddot{P}\ t^3)$$

It can then be shown that

$$t_{bk} \approx k\ P_0 + k^2\ P_0\ \dot{P}_0/2 + 0(k^3\ P) \tag{16}$$

The quantity d(t) can be replaced with the scalar product $-\overline{r}_a(t) \cdot \overline{U}_p(t)$, where $\overline{r}_a(t)$ is the position vector of the antenna relative to the barycenter at time t. The unit vector $\overline{U}_p$ is the direction vector of the pulsar as seen from the barycenter. Referring to Figure 34, note that $|\overline{r}_a| = a \sim 1$ AU, and $R/a >> 1$. Using the facts that

$$Y = -a \cos \theta - d$$

$$2(R-d)Y = X^2 + Y^2$$

and

$$X^2 + Y^2 = Z^2 = d^2 + a^2 + 2ad \cos \theta,$$

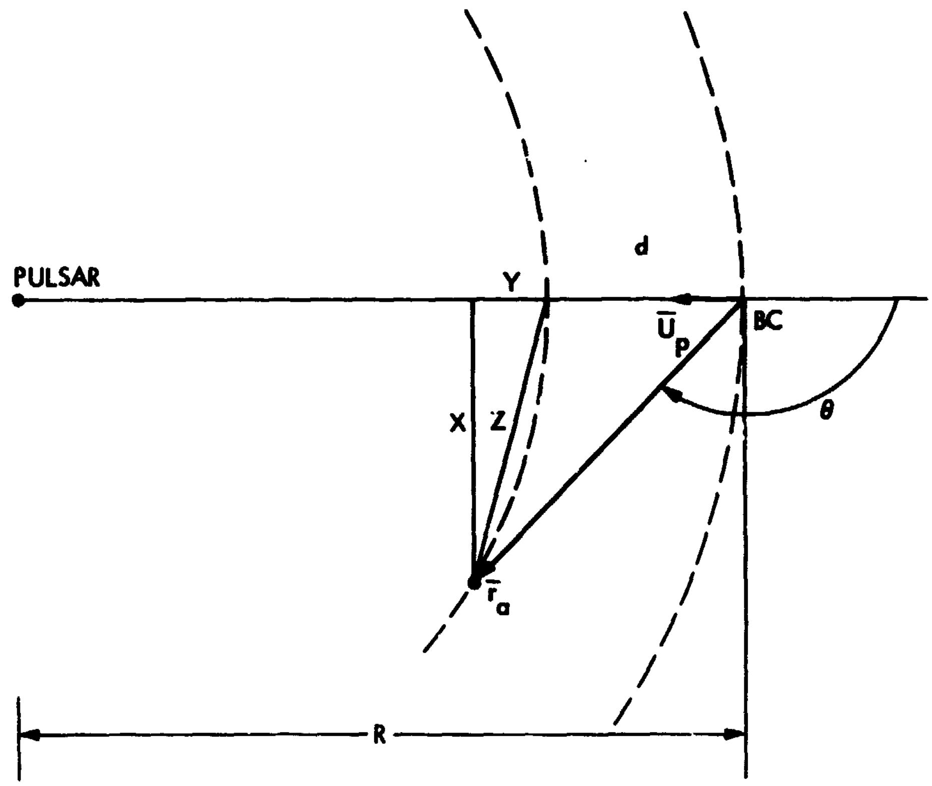


Figure 34. Geometry for Calculating the Phase Drift

the distance d becomes

$$d \approx -a \cos \theta = - \overline{r}_a \cdot \overline{U}_p$$

where $R/a >> 1$. (The smallest value of this ratio is about $10^7$.)

Consider the arrival time obtained if $P(t) = P_a$ over the entire interval of integration. Suppose there is a delay of $\ell$ pulses from the time the timing pulses are started to the time when the data collection is started (usually a few seconds at most). Then M groups of N pulses (usually 500) are superimposed, with n pulses elapsing between groups to allow for a visual display of the progress of the observation. Figure 35 displays the numerology used in counting these pulses. Under the

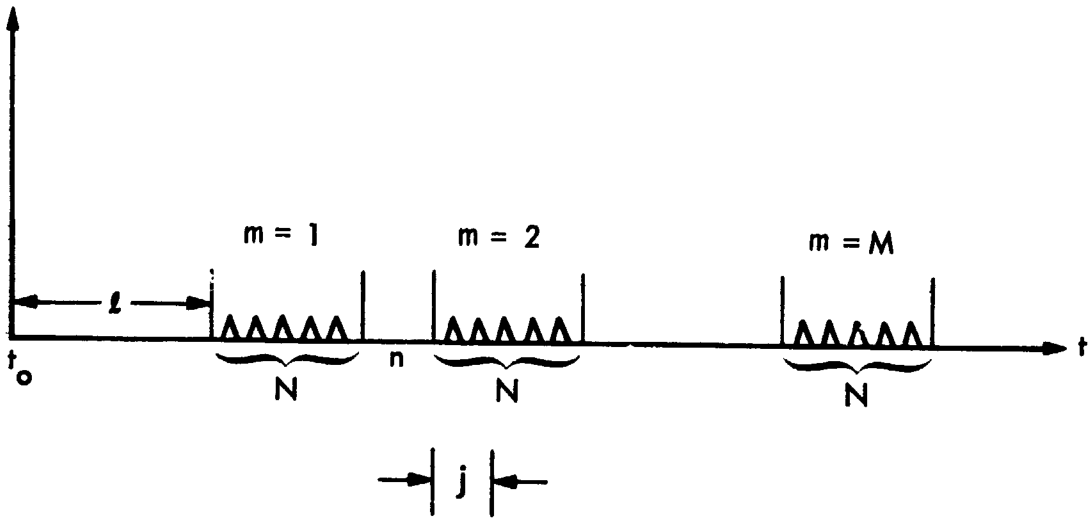


Figure 35. Nomenclature for Enumerating Pulses

assumption of a constant period, the arrival time $t_{ak}$ of the $k^{th}$ pulse after the start epoch $t_0$ is

$$t_{ak} = [\ell + j + (N + n)(m - 1)]\, P_a = kP_a$$

where j is the pulse in question in the $m^{th}$ block of N pulses, and $P_a$ is the assumed constant period. (The synthesizer frequency $f_s$ used in the observation, as per Figure 2, is $10^6/P_a$.)

The mean of the difference $t_k - t_{ak}$ is given by

$$E\left\{t_k - t_{ak}\right\} = \overline{t_k} - \overline{t_{ak}} = \frac{1}{NM} \sum_{m=1}^{M} \sum_{j=1}^{N} (t_k - kP_a)$$

Let $D = \overline{t_k - t_{ak}}$, representing the bias caused by the smearing. Substituting Eqs. (15) and (16) into the expression for D yields

$$D = \frac{(P_0 - P_a)}{NM} \sum_{m=1}^{M} \sum_{j=1}^{N} \{j + \ell + (N + n)(m - 1)\} + \frac{P_0 \dot{P}_0}{2NM} \sum_{m=1}^{M} \sum_{j=1}^{N} \tag{17}$$

$$\{j + \ell + (N + n)(M - 1)\}^2 + \frac{1}{cNM} \sum_{m=1}^{M} \sum_{j=1}^{N} \{d(t_k) - d(t_0)\}$$

The mean of the distances $d(t_k)$ can be replaced by the distance near the midpoint of the range of j, yielding for the third term of Eq. (17),

$$-\frac{1}{cM}\sum_{m=1}^{M}\left\{\bar{r}_a\left[\frac{t_{N+1}}{2} + \ell + (N + n)(m - 1)\right] - \bar{r}_a(t_0)\right\}\cdot \bar{U}_p(t_0)$$

Performing the indicated summations, Eq. (17) becomes

$$\begin{aligned} D = {} & \left[\frac{N + 1}{2} + \ell + \frac{(N + n)(M - 1)}{2}\right] (P_0 - P_a) \\ & + \frac{P_0\dot{P}_0}{2}\left\{\left[\frac{N + 1}{2} + \ell + \frac{(N + n)(M - 1)}{2}\right]^2 + \frac{(N^2 - 1) + (N + n)^2\,(M^2 - 1)}{12}\right\} \\ & - \frac{1}{cM}\sum_{m=1}^{M}\left\{r_a\left[\frac{t_{N+1}}{2} + \ell + (N + n)(m - 1)\right] - \bar{r}_a(t_0)\right\}\cdot \bar{U}_p(t_0) \end{aligned} \qquad (18)$$

It has been assumed that the signal strength is constant over the range of k. Large fluctuations cause Eq. (18) to be in error, and if the drift is large, the results may be rejected.

The expression derived above for the drift is applied to all the data. In all cases, N = 500. The delay $\ell$ is usually 0. The plot time n is equivalent to 30 seconds before Julian date 2440195.5, and 17 seconds thereafter. The number M of 500-pulse integrations varies depending on pulse strength, ranging from the equivalent of a few minutes to over two hours.

The Jet Propulsion Laboratory ephemeris DE 96 is used to compute barycentric positions $\bar{r}_a$. One major export from this observing program is ephemeris independent, geocentric arrival times. However, the drift correction is needed, and is best done by the observer early in the reduction process. The use of a different ephemeris of similar quality will not change the corrections of Eq. (18) significantly. A large drift correction is on the order of a few milliseconds, and a velocity difference between two ephemerides of greater than 0.1 percent would be required to produce a 1 μsec change in the drift estimate. This is usually less than the error estimates encountered in these measurements. Note also that this correction is dependent on a good knowledge of the pulse period and its derivatives. These have been well-determined in a separate data analysis effort.

The sum of the barycentric position vector of the geocenter and the geocentric position of the antenna, $\overline{r}_g$, yields $\overline{r}_a$. The computation of $\overline{r}_g$ is discussed in the next section. The direction vector $\overline{U}_p$ is derived from a model-fitting procedure, which is beyond the scope of this report. All the pulsar positions used here are known to at least 1 arc-sec, an error that will produce a geocentric arrival time error of 0.1 μsec or less.

An example of phase drift and the subsequent correction for the effect is shown in Figure 36. Sixteen groups of 500 pulses of PSR 0833-45 were examined separately to estimate τ. The solid circles represent these estimates relative to the estimate for m = 1. The line through the solid circles represents a fit-by-eye to the linear drift. The triangle is the result of examining the accumulation of the 16 blocks of data. As one would expect in a well-behaved situation, this estimate of τ has drifted about one-half the distance from "0" as the estimate for the m = 16 case alone. This line through the triangle and the zero for this example (0 at m = 1) delineates the hypothetical drift one would find in examining accumulation of the preceding blocks of data. The quantity D, derived from Eq. (18), is the amount the result represented

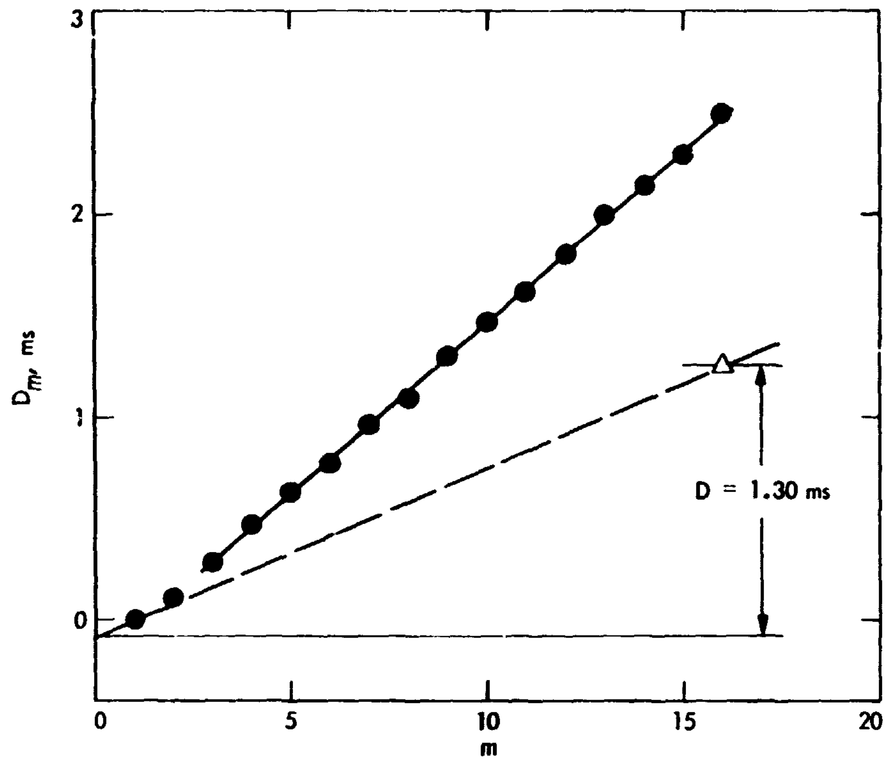


Figure 36. An Example of Drift in the Phase of PSR 0833-45 on 1 Dec. 1968 at $11^h\ 00^m\ 00^s$ (UT)

by the triangle is shifted to correct for drift. Note that by shifting the datum down by D ms, it is nearly in line with the intersection of the dashed line and the m = 0 axis. In a later analysis the resulting $\hat{\tau}$ was found to be only 15 μsec away from the arrival time predicted by a smooth model, which was fitted to several months of data.

B. ANTENNA POSITION

The referral of the measured arrival time to the geocenter requires the addition of the time delay $\overline{r}_g \cdot \overline{U}_{pg}/c$, where $\overline{r}_g$ is the geocentric position of the antenna and $\overline{U}_{pg}$ is the geocentric direction vector of the pulsar. In practice $\overline{U}_{pg} \approx \overline{U}_p$. The coordinate system used here is the right-handed rectangular system (X, Y, Z). The coordinate X is in the direction of $0^h$ Right Ascension (RA) at 1950.0. The station position at a particular UTC epoch is calculated from the antenna coordinates in

Table 5 and the knowledge of the Greenwich Hour Angle (GHA). The station coordinates are a version of Location Set (LS) 44, which are based on the ephemeris DE 96 (Ref. 19). The GHA is computed as outlined in Table 6 (see Ref. 20).

Table 5. Geocentric Antenna Coordinates

| Antenna | West Longitude $\beta$ (deg) | Latitude $\lambda$ (deg) | Radius R (km) |
|---|---|---|---|
| DSS 11 (26m) | 116.849390 | 35.208047 | 6372.011 |
| DSS 12 (34m) | 116.805462 | 35.118665 | 6371.994 |
| DSS 13 (26m) | 116.794863 | 35.066546 | 6372.117 |
| DSS 14 (64m) | 116.889507 | 35.170847 | 6366.227 |
| DSS 62 (26m) | 4.367811 | 40.263145 | 6369.963 |
| DSS 63 (64m) | 4.247991 | 40.241318 | 6370.048 |

Table 6. Relations Used in Computing the GHA of an Observing Station

At the epoch d + SEC/86400,

$$GHA = 100.0755426 + d(0.985647346 + 2.9015 \times 10^{-13} d) + \dot{\theta}\ SEC + \delta\Psi \cos(\varepsilon)\ \text{degrees}$$

where: (1) d = Julian days past 2433282.5

(2) SEC = seconds past $0^h$ on day d

(3) $\dot{\theta} = 4.17807417 \times 10^{-3}/(1 + 5.21 \times 10^{-13}\ d)$ deg/sec

(4) $\delta\Psi$, the nutation in longitude, is taken from ephemeris DE 96

(5) $\dot{\varepsilon} = 4.09205684 \times 10^{-1} + T[-2.28534 \times 10^{-4} + T(-1.5 \times 10^{-8} + 8.7 \times 10^{-9})]$ radians

where T is in Julian centuries of 36525 days past 2433282.5.

The components of the geocentric antenna vector are computed in the 1950.0 coordinate system, requiring rotations for precession and nutation. Considering an antenna at longitude β and latitude λ at a given epoch,

$$\bar{r}_g = \begin{bmatrix} r_{gx} \\ r_{gy} \\ r_{gz} \end{bmatrix} = \begin{bmatrix} P_{11} & P_{12} & P_{13} \\ P_{21} & P_{22} & P_{23} \\ P_{31} & P_{32} & P_{33} \end{bmatrix} \times \begin{bmatrix} 1 & -\delta\Psi\cos(\bar{\varepsilon}) & -\delta\Psi\sin(\bar{\varepsilon}) \\ \Delta\Psi\cos(\bar{\varepsilon}) & 1 & -\delta\varepsilon \\ \Delta\Psi\sin(\bar{\varepsilon}) & \delta\varepsilon & 1 \end{bmatrix}$$

$$\times \begin{bmatrix} r'_{gx} \\ r'_{gy} \\ r'_{gz} \end{bmatrix}$$

where

$$\begin{bmatrix} r'_{gx} \\ r'_{gy} \\ r'_{gz} \end{bmatrix} = \begin{bmatrix} R\cos(\lambda)\cos(GHA - \beta) \\ R\cos(\lambda)\sin(GHA - \beta) \\ R\sin(\lambda) \end{bmatrix}$$

The elements $P_{ij}$ of the precession matrix, given in Table 7, are from Ref. 21. An approximation to the nutation matrix has been used, where $\delta\Psi$ and $\delta\varepsilon$ are taken from the ephemeris DE 96, while $\bar{\varepsilon}$ is computed as in Table 6.

The approximations to the precession and nutation matrices are accurate to a few parts in $10^9$ in both angular position and radial magnitude. Since $|\bar{r}_g| \sim 6 \times 10^3$ km, the corresponding error in arrival time is on the order of picoseconds.

Table 7. Elements of the Precession Matrix

$$P_{11} = 1.0 - T^2(2.9697 \times 10^{-4} + 1.3 \times 10^{-7}T)$$

$$P_{12} = T\left[2.234988 \times 10^{-2} + T(6.76 \times 10^{-6} - 2.21 \times 10^{-6}\ T)\right]$$

$$P_{13} = T\left[9.71711 \times 10^{-3} - T(2.07 \times 10^{-6} + 9.6 \times 10^{-7}T)\right]$$

$$P_{21} = -P_{12}$$

$$P_{22} = 1 - T^2(2.4976 \times 10^{-4} + 1.5 \times 10^{-7}\ T)$$

$$P_{23} = -T^2\ (1.085 \times 10^{-4} + 3 \times 10^{-8}T)$$

$$P_{31} = -P_{13}$$

$$P_{32} = P_{23}$$

$$P_{33} = 1 - T^2\ (4.721 \times 10^{-5} - 2 \times 10^{-8}T)$$

Note: T is in Julian centuries of 36525 days past 2433282.423.

Larger errors appear when referring the arrival times to the solar system barycenter. Since one normally works in 1950.0 coordinates and solves for pulsar positions and proper motions in these coordinates, barycentric arrival times are not highly sensitive to the recent increase in the accepted value of the general precession in longitude by 1.1 arc-sec/century. However, changes in the Earth's barycentric position can vary significantly as ephemerides are improved. For example, the difference in the angular position of Earth in DE 108 and that in DE 96 adds up to about 0.5 arc-sec/century.* In a ten-year observing program, the difference is then 0.05 arc-sec, similar to the errors in pulsar positions derived from the arrival time data.

## C. DISPERSION

Considerable effort was expended in the early observations to obtain one frequency, 2388 MHz. This was not always possible, for several observations occurred at 2295 and 2328 MHz. All observations are now at 2295 MHz. Integration of Eq. (1) provides the corrections in time to be added to an arrival time measured at F MHz to refer it back to 2388 MHz. Performing the integration, the correction $\Delta T_D$ becomes

$$\Delta T_D = \frac{DM}{2.410086 \times 10^{-4}} \left[ \frac{1}{(2388)^2} - \frac{1}{F^2} \right] \text{ sec} \qquad (19)$$

where the values of DM are from Table 4.

In the application of $\Delta T_D$ to PSR 0833-45 it was found that an additional 250 μsec had to be subtracted from the measurement when F = 2295 MHz. No significant addendum was needed when F = 2328 MHz. The average pulse shape must be independent of observing frequency if the correction $\Delta T_D$ is to be perfectly adequate. Most shapes do change significantly with frequency, including that of PSR 0833-45, thus creating the need to measure an addendum to $\Delta T_D$.

## D. DOPPLER DISPERSION

The actual frequency of observation varies with the component of antenna velocity laying along the direction of the pulsar. The measured arrival time then has a varying component since the interstellar medium

*E.M. Standish, private communication.

is dispersive. The Doppler-shifted observing frequency $F_0'$ is related to the mean observing frequency $F_0$ by

$$F_0' = F_0 \left(1 + \frac{\overline{V}_a \cdot \overline{U}_p}{c}\right)$$

where $\overline{V}_a$ is the barycentric velocity of the antenna. In this situation, integration of Eq. 1 leads to a form similar to Eq. (19). Performing that operation,

$$\Delta T_{DD} = \frac{DM}{1.205043 \times 10^{-4} F_0^2} \left[\frac{1}{1 + \frac{\overline{V}_a \cdot \overline{U}_p}{c}} - 1\right]$$

where $\Delta T_{DD}$, the correction for Doppler dispersion is added to the measured arrival time. Using the fact that $|\overline{V}_a/c| < 10^{-4}$, and setting $F_0$ = 2388 MHz, the correction becomes

$$\Delta T_{DD} \approx 1.455220 \times 10^{-3} \, DM\left(\overline{V}_a \cdot \overline{U}_p\right) / c \qquad (20)$$

The magnitude of this yearly oscillation is about 6 μsec for PSR 0833-45 and about 18 μsec for PSR 1933+16. This correction is not small in all cases compared to the measurement accuracy, nor is it small compared to the desired uniformity of the approximation to ephemeris time.

## E. ARRIVAL TIME IN UTC

The epoch at which the data sampling process begins is defined by a 1-sec pulse from the station clock. A sequence of 1-second pulses (clock pulses) is sent continuously via microwave link from the Standards Laboratory at the Goldstone complex to the individual tracking stations. Allowing for the delay over the links, these pulses define a UTC which is within 5 μsec of UTC as disseminated by the National Bureau of

Standards (NBS). The 1-second pulses generated at DSS 14, UT(DSS 14), are kept within 5 μsec of the Standards Laboratory pulses. Therefore, at DSS 14 the 1-sec pulses are assumed to be within 10 μsec of UTC (NBS). The 1-sec pulse used at DSS 13, UT(DSS 13), is frequently synchronized with the Standards Laboratory pulses to within 1 μsec. A piece-wise linear curve approximating the deviation in this 1-sec pulse from UTC(NBS) is used to correct epochs at DSS 13 to UTC (NBS). The correction is at most 100 μsec.

The correction equal to the width of the clock pulse at DSS 14 is subtracted as part of this correction. (See the discussion of system codes 2, 3, and 5, and Fig. 3.) The small correction equal to $P_a/5000$ is then added if appropriate.

## F. CONVERSION FROM COORDINATED UNIVERSAL TIME TO EPHEMERIS TIME

Coordinated Universal Time (UTC) is an approximation to a uniform time based on the rotation of Earth. Several steps are necessary to convert to the truly uniform ephemeris time (ET). Of prime importance is the correction for annual effects due to the orbital motion of the Earth-based clocks about the Sun. The correction ΔET is given in (Ref. 16) as

$$\Delta ET = 0.001658(\sin E + 0.0368) \text{ sec} \qquad (21)$$

where E is the eccentric anomaly of the Earth in a heliocentric orbit. Letting M represent the mean anomaly of Earth and e the orbital eccentricity,

$$\sin E = \sin M (1 + e \cos M)$$

Letting an ET epoch be represented by a Julian ephemeris date (JED) plus the number of seconds (SEC) past $0^h$ ET,

$$M = 358.000682 + 0.9856002628d - T^2(1.55 \times 10^{-4} + 3.33 \times 10^{-6}T) \text{ degrees}$$

$$e = 0.0167301085 - T(4.1926 \times 10^{-5} + 1.26 \times 10^{-7}T)$$

where

$$d = (\text{JED} - 2433282.5 + \text{SEC}/86400) \text{ days}$$

$$T = d/36525 \text{ centuries}$$

(see Ref. 17)

Eq. (21) omits a monthly term of 1.5 μsec, a 12-year term of 21 μsec, and a 29-year term of 5 μsec (Ref. 10).

The ET epoch corresponding to each UTC arrival time, represented by a Julian date JD plus the number of seconds SEC past $0^h$, is computed from

$$\text{ET} - \text{UTC(USNO)} = \begin{cases} \Delta\text{ET} + 38.662738 + 0.002592d \text{ sec; JD} < 2441317.5 \\ \Delta\text{ET} + 32.184 + n \text{ sec; JD} > 2441317.5 \end{cases} \tag{22}$$

where ΔET is computed using Eq. (21), d = JD - 2440000.5 + SEC/86400, n is an integral number of seconds, increasing once or twice a year by 1 second (Ref. 15), and UTC(USNO) is the UTC kept by the U.S. Naval Observatory. The following assumptions and relations were used in computing Eq. (22) before 1 Jan. 1972:

(1) $|\text{UTC(NBS)} - \text{UTC(USNO)}| < 10$ μsec (Refs. 12, 13)

(2) A.1 - UTC(USNO) = 6.5131177 + 0.002592d sec (Ref. 14)

(3) IAT - A.1 = -0.03439 sec (Ref. 15)

(4) ET - IAT = 32.184 sec (Ref. 15)

After Jan. 1972, the appropriate number of integral seconds is added to the UTC epoch to obtain IAT (Ref. 15) under the assumption that |UTC(NBS) - UTC (Bureau de l'Heure)| < 10 μsec (Ref. 12). Then ET is obtained from ET - IAT = 32.184 sec.

G. AN EQUIPMENT IDIOSYNCRASY

The equipment problem of system code 3 requiring a correction of -0.996550 seconds is taken into account along with the corrections discussed above.

H. A TEST OF THE MEASUREMENT CONSISTENCY

The consistency of the measurements is determined by comparing the results using the procedures described earlier in the editing process (Sec. III). This comparison led to the correction of 0.996550 sec for the equipment failure, and the additional 250 μsec correction at 2295 MHz for PSR 0833-45. The question finally arises concerning the consistency of arrival times measured at different stations. Six epochs exist for PSR 0833-45 for which measurements were made at DSS 13 and DSS 14 within 1 day of each other. Results of three of these measurements showed DSS 14 results differing significantly from those at DSS 13. There were, however, serious receiver tuning problems at DSS 14 at two of the three epochs. Of the three results showing agreement, two are presented in Figure 37, where the difference (residual) between the measured and predicted arrival times is presented for each Julian date (JD) of observation (MJD = JD - 2440000.5). The agreement is remarkably good, leading to the conclusion that no systematic differences between DSS 13 and DSS 14 measurements remain in this data set.

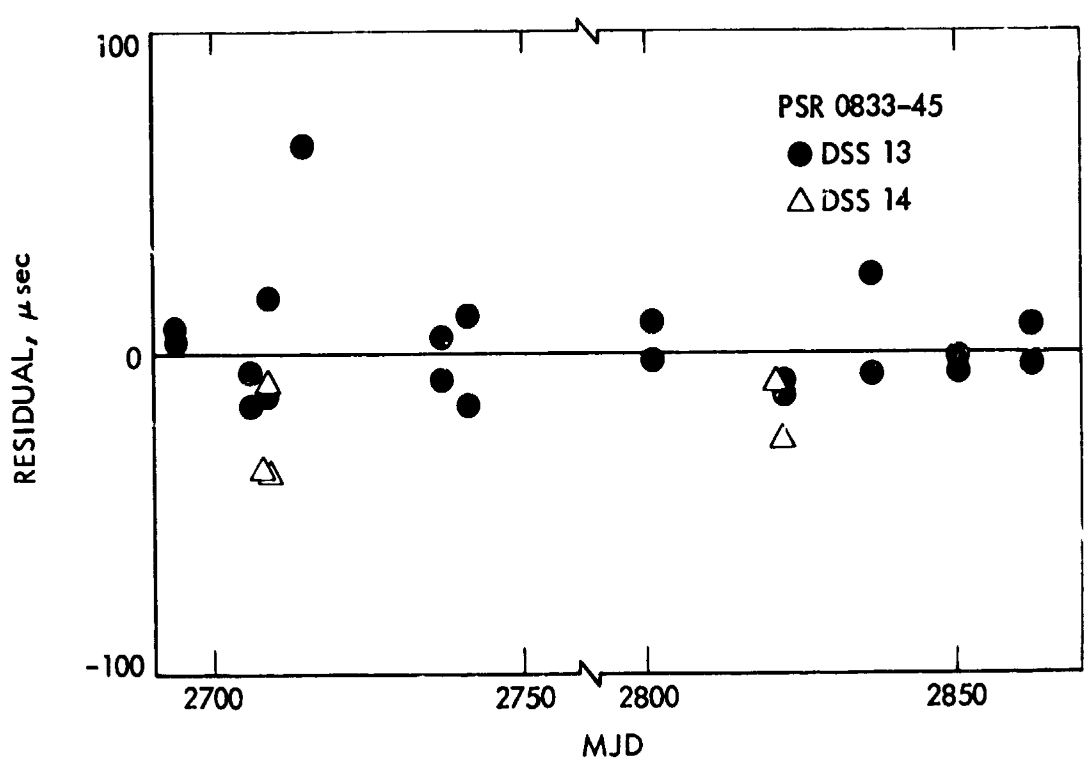


Figure 37. Time-of-arrival Residuals of Measurements Made at DSS-13 and DSS-14 on the Modified Julian Date (MJD) of Observation for PSR 0833-45

# SECTION VII

# THE TABULAR RESULTS

An example of the observational results is presented in Table 8. Columns 1 and 2 list the ephemeris time of the pulse arrival at the geocenter as a Julian ephemeris date and the number of seconds past $0^h$(ET). (Note that no complete removal of the dispersion effect has been applied. That is, these arrival times refer to F = 2388 MHz, not F = ∞.) The estimate of the expected standard deviation of the measurement (defining the 67 percent confidence interval if the measurement errors are Gaussian) appears in Column 3. In Column 4, all of the time conversions from UTC to ET discussed in Section VI are listed. Column 5 contains the applied drift correction, while the configuration code appears in Column 6. Barycentric arrival times are listed in Column 7 for analysts satisfied with the accuracy of DE 96.

## ACKNOWLEDGEMENT

Over the course of ten years many individuals have contributed to the success of this observing program, most of them on the staff of the NASA Deep Space Network. Dedicated, excellent work was and is performed in the collection of the data by G. Birkedahl, R. Genzmer, J. W. Hudson, C. Kodak, C. Mitchell, R. McConahy, D. Rife, L. Skjerve, D. Spitzmesser, L. Wadsworth, G. Wischmeyer, and the staff of DSS 62. Much patient support has been contributed by R. M. Goldstein, R. R. Green, E. B. Jackson and G. S. Levy.

Critical technical support was kindly provided by S. S. Brokl, C. F. Foster, R. R. Green, G. A. Morris, K. I. Moyd, A. G. Slekys, J. Urech, and M. Urech.

Table 8. PSR 0823+26 Biocentric Times-of-Arrival

| MJD | EPHEMERIS TIME SEC PAST 0H ET | σ (μSEC) | ET-UTC (SEC) | DRIFT (μSEC) | SYS CDE | BARYCENTRIC ARRIVAL TIME |
|---|---|---|---|---|---|---|
| 264 | 37339.454552 | 150 | 39.365111 | -1404 | 0 | 37853.397786 |
| 264 | 40939.852707 | 54 | 39.361652 | -1286 | 0 | 41293.654283 |
| 276 | 2139.922026 | 59 | 39.389329 | -732 | 0 | 2549.224551 |
| 276 | 5439.639974 | 156 | 39.392411 | -1139 | 0 | 5848.865729 |
| 276 | 30939.589416 | 54 | 39.399016 | -949 | 0 | 31347.767834 |
| 283 | 1839.772454 | 40 | 39.407353 | -11 | 0 | 2214.028455 |
| 283 | 5439.463046 | 77 | 39.411178 | 26 | 0 | 5813.432579 |
| 283 | 9039.584439 | 13 | 39.414541 | -6 | 0 | 9413.457270 |
| 290 | 1839.507548 | 58 | 39.427318 | 32 | 0 | 2173.349422 |
| 290 | 5439.529535 | 16 | 39.430990 | 9 | 0 | 5772.813610 |
| 290 | 9039.782508 | 27 | 39.434012 | -4 | 0 | 9372.809468 |
| 290 | 12639.504558 | 51 | 39.436219 | -42 | 0 | 12972.272477 |
| 297 | 5439.792447 | 23 | 39.450641 | -5 | 0 | 5727.359923 |
| 297 | 9039.532058 | 22 | 39.453301 | -21 | 0 | 9325.823947 |
| 303 | 79239.529201 | 57 | 39.457139 | 35 | 0 | 79478.210658 |
| 303 | 82839.832748 | 43 | 39.461303 | 27 | 0 | 83078.205944 |
| 304 | 3639.908226 | 8 | 39.468632 | 19 | 0 | 3877.654574 |
| 304 | 7539.529311 | 23 | 39.471489 | 24 | 0 | 7776.931364 |
| 310 | 82839.519275 | 27 | 39.481255 | 34 | 0 | 83024.794362 |
| 311 | 7239.722479 | 25 | 39.490392 | -11 | 0 | 7423.717370 |
| 324 | 25239.959177 | 195 | 39.517531 | -50 | 0 | 25315.465774 |
| 332 | 6940.054546 | 25 | 39.545251 | -158 | 0 | 6950.931182 |
| 332 | 10939.733435 | 39. | 39.546097 | -104 | 0 | 10950.217859 |
| 332 | 14139.695332 | 25 | 39.545037 | -90 | 0 | 14149.859461 |
| 338 | 7240.044201 | 13 | 39.561746 | -92 | 0 | 7200.124622 |
| 338 | 10939.560054 | 36 | 39.541200 | -101 | 0 | 10799.589946 |
| 338 | 92939.954352 | 10 | 39.559963 | -89 | 0 | 82792.596500 |
| 345 | 79239.877574 | 39 | 39.575297 | -76 | 0 | 79134.409741 |
| 345 | 82939.686577 | 51 | 39.579184 | -85 | 0 | 82733.873999 |
| 346 | 7239.643949 | 13 | 39.582161 | -91 | 0 | 7132.737249 |
| 352 | 75520.039979 | 51 | 39.593141 | -910 | 0 | 75357.897343 |
| 352 | 79539.651757 | 18 | 39.596347 | -485 | 0 | 79377.113437 |
| 352 | 53140.010154 | 149 | 39.598551 | -253 | 0 | 52977.107997 |
| 352 | 84339.342955 | 46 | 39.599251 | -357 | 0 | 84176.929557 |
| 359 | 69040.009998 | 8 | 39.604965 | -1 | 0 | 68523.548123 |
| 359 | 72040.093939 | 6 | 39.608537 | -39 | 0 | 71923.366835 |
| 359 | 75939.725470 | 16 | 39.612205 | -33 | 0 | 75722.653721 |
| 359 | 79239.658476 | 18 | 39.614897 | -57 | 0 | 79022.293182 |
| 366 | 72040.037218 | 72 | 39.628015 | -51 | 0 | 71771.556789 |
| 366 | 75639.859190 | 131 | 39.631351 | -60 | 0 | 75371.020937 |
| 366 | 79240.151305 | 43 | 39.633942 | -81 | 0 | 78971.015538 |
| 381 | 3640.073438 | 16 | 39.670276 | -66 | 0 | 3278.525561 |
| 391 | 57640.009595 | 49 | 39.682781 | -325 | 0 | 57222.027595 |
| 394 | 54839.794743 | 3 | 39.698615 | -25 | 12 | 54407.550878 |

| MJD | EPHEMERIS TIME SEC PAST 0H ET | σ (μSEC) | ET-UTC (SEC) | DRIFT (μSEC) | SYS CDE | BARYCENTRIC ARRIVAL TIME |
|---|---|---|---|---|---|---|
| 394 | 68439.960254 | 5 | 39.702037 | -47 | 12 | 68007.545592 |
| 405 | 61240.157935 | 63 | 39.734421 | -3 | 12 | 60759.355555 |
| 405 | 68439.839075 | 33 | 39.740703 | -31 | 12 | 67959.425595 |
| 414 | 51240.056941 | 24 | 39.751135 | -12 | 12 | 50747.024929 |
| 414 | 64840.129777 | 11 | 39.754560 | -27 | 0 | 64347.020024 |
| 414 | 68440.190160 | 7 | 39.756954 | -44 | 12 | 67947.014907 |
| 471 | 51340.028659 | 20 | 39.900565 | 15 | - | 50372.219317 |
| 478 | 43240.082258 | 43 | 39.912363 | 15 | 0 | 42314.395259 |
| 478 | 46540.336417 | 15 | 39.916055 | 3 | 0 | 46515.421303 |
| 493 | 39640.198256 | 32 | 39.950915 | 77 | 0 | 39421.871755 |
| 493 | 43240.403111 | 32 | 39.954684 | 25 | 0 | 43022.397492 |
| 499 | 36040.294461 | 25 | 39.964023 | 25 | 0 | 35555.911533 |
| 499 | 39640.484830 | 23 | 39.968004 | 12 | 0 | 39459.437229 |
| 506 | 36040.390146 | 5 | 39.994544 | -525 | 0 | 35325.440135 |
| 506 | 39640.037592 | 26 | 39.998441 | -535 | 0 | 39525. 35234 |
| 513 | 34240.078079 | 15 | 40.001937 | 47 | 0 | 34155 033755 |
| 513 | 37840.248849 | 15 | 40.005844 | -53 | 0 | 37755.529355 |
| 520 | 28840.430239 | 5 | 40.015794 | 55 | 0 | 28544.596735 |
| 520 | 32440.058432 | 22 | 40.019932 | 42 | 0 | 32444.559777 |
| 524 | 28840.223673 | 44 | 40.027202 | 37 | 0 | 28875.707065 |
| 524 | 32440.393751 | 34 | 40.031393 | 12 | 0 | 32479.232927 |
| 524 | 36040.553296 | 63 | 40.035075 | 27 | 0 | 36073.758254 |
| 551 | 30640.230304 | 5 | 40.106311 | -33 | 0 | 30935.735055 |
| 551 | 34420.330701 | 9 | 40.109327 | -48 | 0 | 34577.175405 |
| 551 | 48640.250006 | 14 | 40.111103 | -62 | 0 | 48933.323159 |
| 578 | 43240.218028 | 12 | 40.191151 | -79 | 0 | 43555.537454 |
| 613 | 32440.642039 | 26 | 40.273715 | -115 | 0 | 32325.057475 |
| 613 | 36040.665029 | 37 | 40.272067 | -119 | 0 | 35525.052633 |
| 613 | 39640.658398 | 20 | 40.269485 | -82 | 0 | 40125.057905 |
| 652 | 19300.501394 | 16 | 40.376002 | -142 | 0 | 19553.400855 |
| 652 | 23440.458964 | 23 | 40.375255 | -112 | 0 | 23793.075912 |
| 653 | 25960.713441 | 22 | 40.376555 | -37 | 0 | 26307.225392 |
| 678 | 14740.531334 | 7 | 40.443212 | -70 | 0 | 14911.043607 |
| 678 | 17920.536400 | 29 | 40.442432 | -122 | 0 | 18030.755237 |
| 678 | 23440.356098 | 23 | 40.439003 | 75 | 0 | 23510.573107 |
| 708 | 10660.754316 | 11 | 40.519847 | -115 | 0 | 10551.522456 |
| 708 | 14200.606820 | 26 | 40.518044 | -97 | 0 | 14121.122434 |
| 714 | 17440.739522 | 14 | 40.529865 | -59 | 0 | 17311.254755 |
| 730 | 10840.933590 | 9 | 40.573235 | -65 | 0 | 10557.572021 |
| 737 | 8920.973639 | 25 | 40.591375 | -70 | 0 | 8515.543253 |
| 745 | 1120.916371 | 25 | 40.553805 | -23 | 0 | 559.759220 |
| 793 | 75641.255830 | 59 | 40.740413 | -71 | 0 | 75139.824110 |
| 793 | 79120.751711 | 20 | 40.738959 | -70 | 0 | 78515.359547 |
| 793 | 92600.538079 | 22 | 40.736610 | -33 | 0 | 92038.425703 |

ORIGINAL PAGE IS OF POOR QUALITY

TABLE 8 (CONTINUED). PSR 0823+26

| | | | | | | | | | | | | | | |
|---|---|---|---|---|---|---|---|---|---|---|---|---|---|---|
| 921 | 68449.353852 | 272 | 40.912299 | -60 | 0 | 67999.337469 | • | 1422 | 12882.317325 | 5 | 42.206381 | -89 | 0 | 12943.389737 |
| 921 | 71921.287657 | 38 | 40.811001 | -59 | 0 | 71479.934327 | • | 1422 | 16062.340103 | 7 | 42.205116 | -110 | 0 | 16123.503023 |
| 942 | 47749.923931 | 18 | 40.861259 | -94 | 0 | 47405.964203 | • | 1422 | 19842.597596 | 7 | 42.202639 | -81 | 0 | 19903.492577 |
| 942 | 52061.235131 | 38 | 40.863652 | -22 | 0 | 51729.595303 | • | 1450 | 3642.320059 | 12 | 42.206445 | -93 | 0 | 3471.505955 |
| 942 | 55759.894117 | 10 | 40.865665 | -56 | 0 | 55469.5198.5 | • | 1450 | 7122.707136 | 34 | 42.205776 | -105 | 0 | 6951.372772 |
| 969 | 45041.064463 | 31 | 40.932897 | -26 | 0 | 44910.240000 | • | 1450 | 10602.553206 | 15 | 42.204135 | -105 | 0 | 10431.105812 |
| 969 | 48641.246238 | 18 | 40.935017 | -45 | 0 | 48510.755045 | • | 1475 | 84762.572027 | 10 | 42.205887 | -177 | 0 | 84424.472445 |
| 869 | 57221.192647 | 5 | 40.925975 | -91 | 0 | 57091.533143 | • | 1476 | 3522.533266 | 13 | 42.204075 | -83 | 0 | 3159.275375 |
| 909 | 28841.352361 | 63 | 41.030667 | -24 | 0 | 29043.531073 | • | 1476 | 7242.715003 | 6 | 42.201603 | -60 | 0 | 6589.000444 |
| 909 | 32321.104261 | 13 | 41.034137 | -59 | 0 | 32523.897402 | • | 1505 | 83383.535265 | 37 | 43.202917 | -31 | 0 | 82902.173042 |
| 909 | 36041.223608 | 18 | 41.037082 | -34 | 0 | 36244.352567 | • | 1505 | 86323.470093 | 15 | 43.200972 | -55 | 0 | 85942.045031 |
| 909 | 39641.424477 | 58 | 41.039105 | -72 | 0 | 39844.875714 | • | 1546 | 4123.225310 | 10 | 43.197239 | -20 | 0 | 3541.589613 |
| 982 | 34361.563150 | 34 | 41.225835 | 79 | 0 | 34844.359582 | • | 1540 | 72223.350013 | 15 | 43.203365 | -44 | 0 | 71745.407549 |
| 982 | 36701.275355 | 13 | 41.227499 | -24 | 0 | 37184.065220 | • | 1540 | 75463.493247 | 4 | 43.201822 | -35 | 0 | 74955.616525 |
| 1009 | 25421.549816 | 36 | 41.300478 | -65 | 0 | 24819.701183 | • | 1540 | 79243.271617 | 149 | 43.199083 | -17 | 0 | 78755.596477 |
| 1010 | 29381.680718 | 40 | 41.300961 | -36 | 0 | 29774.599402 | • | 1549 | 40483.616120 | 31 | 43.159107 | 23 | 0 | 40130.595805 |
| 1030 | 27701.575394 | 105 | 41.350650 | -46 | 0 | 27971.902892 | • | 1549 | 66823.722943 | 34 | 43.202263 | [illegible] | 0 | 66472.549835 |
| 1030 | 30341.823738 | 71 | 41.348327 | -87 | 0 | 30611.934824 | • | 1569 | 70303.545275 | 84 | 43.200245 | -27 | 0 | 69952.715652 |
| 1032 | 27341.531839 | 20 | 41.355758 | -64 | 0 | 27597.571295 | • | 1597 | 59683.526153 | 27 | 43.202335 | -11 | 0 | 59534.733895 |
| 1032 | 30581.480979 | 22 | 41.352796 | -62 | 0 | 30837.245921 | • | 1597 | 63223.223093 | 35 | 43.200388 | -15 | 0 | 63074.825359 |
| 1051 | 14441.711589 | 16 | 41.409706 | -113 | 0 | 14550.313520 | • | 1597 | 66703.491880 | 50 | 43.197655 | -8 | 0 | 66555.423157 |
| 1051 | 17921.579979 | 18 | 41.408337 | -108 | 0 | 18029.849226 | • | 1549 | 36403.309637 | 3 | 43.201550 | -201 | 1 | 36511.544545 |
| 1051 | 21581.890096 | 20 | 41.405938 | -79 | 0 | 21689.809353 | • | 1549 | 39643.283961 | 5 | 43.204348 | 1 | 1 | 39995.735150 |
| 1079 | 5801.605579 | 5 | 41.482131 | -72 | 0 | 5576.269156 | • | 1559 | 40483.258570 | 11 | 43.204312 | 23 | 1 | 40825.329374 |
| 1079 | 9701.793500 | 18 | 41.481122 | -35 | 0 | 9576.087472 | • | 1572 | 40843.667669 | 20 | 43.204027 | 7 | 1 | 41255.075934 |
| 1079 | 12641.925948 | 18 | 41.479656 | -73 | 0 | 12515.942320 | • | 1572 | 41203.435970 | 25 | 43.203899 | 12 | 1 | 41515.553491 |
| 1107 | 56021.616248 | 28 | 41.556485 | -137 | 0 | 85683.501569 | • | 1588 | 31544.717591 | 11 | 44.205066 | 8 | 1 | 32013.551654 |
| 1108 | 64951.657450 | 1 | 41.546163 | -18 | 0 | 64618.857409 | • | 1588 | 31844.532015 | 11 | 44.205094 | 12 | 1 | 32313.504546 |
| 1108 | 68441.971954 | [illegible] | 41.550005 | -42 | 0 | 68098.323919 | • | 1596 | 26444.473627 | 6 | 44.204503 | -5 | 1 | 26929.159459 |
| 1135 | 69251.820224 | 65 | 41.625340 | -48 | 0 | 68812.983178 | • | 1596 | 27044.641023 | 14 | 44.204704 | 4 | 1 | 27529.335523 |
| 1135 | 79192.150905 | 16 | 41.629092 | -85 | 0 | 78712.971113 | • | 1596 | 27704.241604 | 15 | 44.204854 | 25 | 1 | 28157.345533 |
| 1135 | 82661.805704 | 9 | 41.627172 | -94 | 0 | 89192.505904 | • | 1715 | 18644.471207 | 5 | 44.203353 | -20 | 1 | 19125.179190 |
| 1163 | 32081.909999 | 15 | 41.695659 | -148 | 0 | 64582.378544 | • | 1715 | 19004.264987 | 13 | 44.203567 | -14 | 1 | 19494.365398 |
| 1153 | 56461.930059 | 20 | 41.695951 | -84 | 0 | 65963.043956 | • | 1773 | 8204.479004 | 9 | 44.205909 | -114 | 1 | 8353.575176 |
| 1153 | 75541.716352 | 30 | 41.698926 | -66 | 0 | 75142.926509 | • | 1773 | 9104.559441 | 9 | 44.206214 | -105 | 1 | 9253.574257 |
| 1192 | 55302.197767 | 15 | 41.770944 | -45 | 0 | 54886.200954 | • | 1773 | 9404.409792 | 20 | 44.206300 | -100 | 1 | 9553.397170 |
| 1219 | 43122.153645 | 36 | 41.835404 | -20 | 0 | 42871.909145 | • | 1787 | 12824.729429 | 23 | 44.206309 | -32 | 2 | 12995.572794 |
| 1219 | 51481.937909 | 18 | 41.843045 | -21 | 0 | 61233.256650 | • | 1787 | 13184.551651 | 24 | 44.205207 | -25 | 2 | 13245.465045 |
| 1219 | 64561.908892 | 18 | 41.841731 | -38 | 0 | 64413.510455 | • | 1717 | 13484.403570 | 37 | 44.206111 | -21 | 2 | 13545.252809 |
| 1279 | 32742.233255 | 9 | 41.994583 | -69 | 0 | 32992.190895 | • | 1598 | 44.327568 | 11 | 44.205595 | -6 | 2 | -67.154509 |
| 1279 | 38142.290106 | 6 | 41.998005 | -28 | 0 | 38382.713209 | • | 1598 | 464.550910 | 24 | 44.205733 | -2 | 2 | 353.125303 |
| 1279 | 46782.273270 | 51 | 41.998915 | -78 | 0 | 47023.447718 | • | 1598 | 884.442724 | 44 | 44.205836 | 32 | 2 | 772.990141 |
| 1305 | 21042.413902 | 16 | 42.065733 | -108 | 0 | 21459.141823 | • | 1545 | 83684.403349 | 4 | 44.205379 | -7 | 1 | 83257.442972 |
| 1305 | 39762.594099 | 6 | 42.074672 | -84 | 0 | 40180.257325 | • | 1545 | 93984.243997 | 4 | 44.205317 | -5 | 1 | 93597.265773 |
| 1305 | 43242.491121 | 15 | 42.073371 | -88 | 0 | 43560.353882 | • | 154[illegible] | 94254.615563 | 4 | 44.205245 | -2 | 1 | 83597.513451 |
| 1337 | 32442.311509 | 8 | 42.205380 | -111 | 0 | 32930.661474 | • | 1575 | 5924.704830 | 15 | 44.193529 | -4 | 2 | 5430.524417 |
| 1337 | 35922.365894 | 22 | 42.204111 | -123 | 0 | 36410.725171 | • | 1595 | 63714.277968 | 9 | 44.202503 | 21 | 2 | 63217.455035 |
| 1337 | 39402.420350 | 10 | 42.201932 | -117 | 0 | 39890.734813 | • | 1595 | 64304.3[illegible]4106 | 14 | 44.202792 | 50 | 2 | 63507.543750 |
| 1393 | [illegible]0352.577521 | 16 | 42.205077 | -46 | 0 | 20563.590762 | • | 1395 | 52654.536475 | 5 | 44.200825 | 15 | 2 | 52337.032533 |
| 1393 | [illegible]122.513819 | 9 | 42.204663 | -79 | 0 | 23909.665200 | • | 1345 | 53274.538237 | 15 | 44.201191 | 24 | 2 | 52927.125255 |
| 1393 | 27102.327597 | 39 | 42.[illegible]2275 | -77 | 0 | 27383.206343 | • | 1383 | 69243.548622 | 7 | 44.203655 | 54 | 2 | [illegible] |

TABLE 8 (CONTINUED). PSR 0923+26

| | | | | | | | | | | | | | | |
|---|---|---|---|---|---|---|---|---|---|---|---|---|---|---|
| 1952 | 50424.249952 | 7 | 44.203457 | 69 | 2 | 50441.17886 | • | 2585 | 62155.441375 | 155 | 46.202031 | 12 | 0 | 61944.056405 |
| 2057 | 20235.504324 | 16 | 45.198086 | 3 | 2 | 20695.109415 | • | 2585 | 63905.400748 | 16 | 45.201098 | 10 | 0 | 63594.202607 |
| 2050 | 20895.622771 | 29 | 45.198687 | 15 | 2 | 21355.2[illegible] | • | 2709 | 58575.424169 | 15 | 45.200376 | 15 | 0 | 58552.135351 |
| 2079 | 14925.519250 | 37 | 45.200320 | -6 | 0 | 15407.9[illegible]489 | • | 2709 | 60316.[illegible]96019 | 73 | 45.199797 | 15 | 0 | 60302.170555 |
| 2079 | 16125.359592 | 18 | 45.2[illegible]355 | -36 | 0 | 16607.66[illegible]57 | • | 2716 | 58906.627264 | 15 | 45.199692 | 27 | 0 | 55952.224891 |
| 2123 | 555.542516 | 24 | 45.198777 | -15 | 0 | 835.[illegible]03 | • | [illegible]16 | 60356.247214 | 47 | 45.195543 | 16 | 0 | 60401.357533 |
| 2123 | 2085.314427 | 31 | 45.200219 | -22 | 0 | 2335.[illegible] | • | 2751 | 46955.347637 | 134 | 45.202692 | 9 | 0 | 47252.765901 |
| 2135 | 16095.357557 | 9 | 45.206479 | -36 | 0 | 16595.[illegible]6 | • | 2751 | 48766.211403 | 205 | 46.201682 | 6 | 0 | 49307.765485 |
| 2135 | 17565.4[illegible]7317 | 5 | 45.205081 | -48 | 0 | 18068.[illegible]4507 | • | 2763 | 44355.211175 | 52 | 46.202736 | -24 | 0 | 44753.232294 |
| 2149 | 12705.717093 | 35 | 45.206552 | -40 | 0 | 12796.524200 | • | [illegible]65 | 46695.257549 | 47 | 45.201273 | -41 | 0 | 47033.443059 |
| 2177 | 7155.659570 | 134 | 45.206002 | -38 | 0 | 7042.4238 | | [illegible]01 | 92477.294254 | 27 | 47.205220 | -60 | 0 | 32953.519545 |
| 2177 | 9225.700450 | 214 | 45.205268 | -33 | 0 | 9082.27945 | • | 2956 | 91327.319750 | [illegible]5 | 47.192020 | 23 | 0 | 91593.513559 |
| 2195 | 7755.326558 | 56 | 45.202845 | -17 | 0 | 7484.358886 | • | 2962 | 2017.656230 | [illegible] | 47.200727 | -47 | 0 | 2245.529178 |
| 2198 | 8985.249558 | 57 | 45.201989 | -32 | 0 | 8654.151036 | • | 2962 | 4357.538993 | 16 | 47.202675 | -45 | 0 | 4585.509035 |
| 2226 | 45.377503 | 22 | 43.202860 | -25 | 0 | -404.553621 | • | 2965 | 79787.654105 | 294 | 47.201941 | -39 | 0 | 79555.592930 |
| 2226 | 1845.453479 | 11 | 45.201651 | -23 | 0 | 1395.444675 | • | 2965 | 81857.674252 | 39 | 47.203487 | -37 | 0 | 81755.514435 |
| 2239 | 92305.255071 | 78 | 45.202607 | -18 | 0 | 92415.090872 | • | 2919 | 71137.700371 | 15 | [illegible]7.196666 | -24 | 0 | 70595.793280 |
| 2239 | 94445.335570 | 159 | 45.201473 | -21 | 0 | 94156.124779 | • | 2947 | 64227.657051 | [illegible] | [illegible]195653 | -13 | 0 | 63512.545205 |
| 2268 | 74955.358413 | 32 | 45.202853 | -10 | 0 | 73601.125414 | • | 2947 | 65707.249258 | [illegible]2 | [illegible]197155 | -20 | 0 | 65292.325151 |
| 2265 | 76725.554207 | 10 | 45.201442 | -10 | 0 | 76241.155243 | • | 2952 | 64137.403691 | 37 | [illegible]196650 | -15 | 0 | 63700.033049 |
| 2294 | 70565.336332 | 16 | 45.200957 | 15 | 0 | 70161.995547 | • | 2952 | 65597.655422 | 22 | 47.198385 | -17 | 0 | 65460.232142 |
| 2294 | 72945.[illegible]7424 | 18 | 45.199938 | 4 | 0 | 71662.174217 | • | 2975 | 76727.702636 | 15 | 47.204462 | -14 | 0 | 76225.017353 |
| 2321 | 56765.615957 | 18 | 45.195576 | 14 | 0 | 66564.673557 | • | 2975 | 78457.676632 | 29 | 47.203964 | -17 | 0 | 77957.355921 |
| 2336 | 53095.320577 | 2 | 45.203390 | 36 | 2 | 53015.755317 | • | 2989 | 73147.234446 | 231 | 47.204144 | -7 | 0 | 72545.729815 |
| 2335 | 61755.373443 | 52 | 45.199993 | 40 | 0 | 61575.665481 | • | 2989 | 74917.498556 | 166 | 47.203667 | -7 | 0 | 74415.011575 |
| 2336 | 63495.737154 | 23 | 45.195676 | 27 | 0 | 63416.699258 | • | 3002 | 66847.459636 | 52 | 47.204056 | -19 | 0 | 66369.515837 |
| 2364 | 35185.426275 | 20 | 45.200408 | -40 | 0 | 55342.677[illegible]33 | • | 3017 | 67607.443507 | 8 | 47.203277 | 0 | 0 | 67153.525052 |
| 2364 | 55545.697528 | 11 | 45.197500 | 7 | 0 | 58823.273692 | • | 3017 | 69357.456991 | 7 | 47.202644 | -3 | 0 | 68933.542527 |
| 2402 | 19705.205145 | 22 | 45.194216 | 18 | 0 | 20313.046342 | • | 3045 | 66347.531277 | 15 | 47.200361 | [illegible] | 0 | 66034.510007 |
| 2402 | 22545.625541 | 52 | 45.195937 | 16 | 0 | 22953.610092 | • | 3045 | 68387.273922 | 31 | 47.199330 | 13 | 0 | 69134.367142 |
| 2430 | 25341.631940 | 14 | 46.204483 | -1 | 3 | 25527.676664 | • | 3059 | 54547.644563 | 30 | 47.199236 | 12 | 0 | 64404.049824 |
| 2430 | 25451.534555 | 16 | 46.204597 | 5 | 3 | 26137.552055 | • | 3059 | 56347.472557 | 20 | 47.197760 | 1 | 0 | 66204.047625 |
| 2430 | 26255.564445 | 18 | 46.204[illegible]5 | 3 | 3 | 26752.617063 | • | 3084 | 59547.247694 | 15 | 47.198708 | 22 | 0 | 59514.945800 |
| 2450 | 35955.720154 | 30 | 45.200974 | -10 | 3 | 37407.155324 | • | 3084 | 61317.355928 | 4 | 47.197139 | 43 | 0 | 61355.225634 |
| 245[illegible] | 37591.655271 | 12 | 46.200461 | -12 | 3 | 38062.137529 | • | 3105 | 58007.511972 | 20 | 47.195993 | -4 | 0 | 58244.506135 |
| 2522 | 20295.594939 | 48 | 46.201375 | -20 | 3 | 20319.523438 | | 3105 | 60307.293323 | 42 | 47.193595 | 15 | 0 | 60544.455555 |
| 2522 | 20700.605530 | 44 | 46.200851 | -19 | 3 | 20924.470915 | • | 3122 | 45527.395247 | 61 | 47.202855 | 25 | 3 | 45979.172765 |
| 2532 | 71605.340219 | 51 | 46.191905 | -21 | 0 | 71540.746522 | • | 3122 | 46157.245192 | 18 | 47.202534 | 24 | 3 | 46505.055314 |
| 2532 | 73955.330593 | 24 | 46.194545 | -25 | 0 | 73590.505632 | • | 3122 | 46757.350398 | 18 | 47.202201 | 23 | 3 | 47105.242257 |
| 2555 | 75136.338011 | 26 | 46.203083 | -18 | 0 | 77556.8377[illegible] | • | [illegible]163 | 27602.618551 | 14 | 45.205365 | 7 | 3 | 28057.545341 |
| 2563 | 55420.707411 | 6 | 46.205984 | -18 | 3 | 85114.391248 | • | [illegible]17 | 22845.554850 | 4 | 45.205252 | -14 | 5 | 23147.758656 |
| 2563 | 56010.315370 | 7 | 45.205952 | -17 | 3 | 55703.944484 | • | 3217 | 23475.49[illegible]032 | 5 | 45.204945 | -19 | 5 | 23777.552041 |
| 2559 | 4055.345524 | 14 | 46.204115 | -12 | 3 | 3745.270667 | • | 3217 | 23835.312546 | 5 | 45.204752 | -15 | 5 | 24137.433555 |
| 2559 | 4705.734958 | 45 | 46.203784 | -16 | 3 | 4365.512301 | • | 3245 | 52574.325234 | 25 | 45.203392 | -37 | 4 | 52/54.35554[illegible] |
| 2510 | 76655.400502 | 3[illegible] | 45.204459 | -16 | 0 | 74157.738511 | • | 3245 | 54755.350120 | 52 | 45.204450 | 45 | 4 | 54565.231397 |
| 2510 | 78405.535535 | 20 | 45.203353 | -17 | 0 | 77907.855026 | • | 3321 | 75811.227272 | 50 | 45.204922 | 35 | 4 | 75357.422931 |
| 2529 | 73306.434417 | 25 | 45.203652 | 0 | 0 | 72512.711942 | • | 3309 | 9059.535544 | 3 | 45.192551 | 413 | 5 | 5551.359744 |
| 2529 | 74755.701234 | 24 | 45.203130 | -11 | 0 | 74263.005647 | • | 3309 | 9645.237658 | 4 | 45.191535 | 412 | 5 | 9170.951365 |
| 2539 | 75535.435511 | 232 | 45.200437 | 4 | 0 | 74165.751944 | • | 3344 | 55942.514551 | 14 | 45.200550 | -29 | 4 | 59454.545015 |
| 2539 | 77505.585953 | 24 | 45.197769 | 19 | 0 | 77035.054333 | • | 3344 | 51152.229232 | 3 | 44.[illegible]72009 | -13 | 4 | 50574.435959 |
| 2550 | 55445.584732 | 22 | 45.203185 | -6 | 0 | 58015.139601 | • | 3387 | 73298.400508 | 02 | 45.199545 | -15 | 4 | 72535.[illegible]30705 |

TABLE 8 (CONTINUED). PSR 0923+26

| | | | | | | | | | | | | | | |
|---|---|---|---|---|---|---|---|---|---|---|---|---|---|---|
| 3397 | 75545.672177 | 56 | 48.197649 | 3 | 4 | 75145.396854 | • | 3549 | 27199.233504 | 9 | 49.205862 | -6 | 5 | 27659.621832 |
| 3435 | 56631.278057 | 13 | 49.195133 | 20 | 4 | 64577.020570 | • | 3549 | 27519.231557 | 11 | 49.205784 | 5 | 5 | 27979.539528 |
| 3435 | 68555.445559 | 46 | 48.193130 | 24 | 4 | 68504.375026 | • | 3533 | 51357.651872 | 76 | 49.202721 | -28 | 4 | 81244.446317 |
| 3462 | 5.153.315025 | 104 | 48.200071 | -40 | 4 | 55325.135197 | • | 3547 | 54935.718833 | 35 | 49.205685 | -25 | 4 | 84574.392173 |
| 3462 | 58597.265977 | 51 | 48.197027 | 7 | 4 | 58863.414443 | • | 3575 | 78431.658201 | 24 | 49.205257 | -29 | 4 | 75025.735524 |
| 3455 | 55784.569613 | 59 | 49.195065 | 5 | 4 | 56121.572003 | • | 3710 | 69528.402898 | 69 | 49.204142 | -13 | 4 | 69023.582972 |
| 3455 | 59589.665412 | 24 | 48.191932 | 7 | 4 | 59025.974503 | • | 3710 | 71111.370993 | 37 | 49.204437 | -21 | 4 | 70606.552044 |
| 3486 | 42598.272902 | 71 | 45.204003 | 20 | 5 | 42940.457232 | • | 3781 | 74625.231148 | 31 | 49.195725 | 1 | 4 | 74219.029809 |
| 3502 | 13939.531295 | 16 | 45.199781 | 13 | 5 | 14361.500768 | • | 3751 | 76265.405992 | 69 | 49.197292 | -3 | 4 | 75959.300142 |
| 3504 | 40079.499684 | 50 | 45.203976 | 17 | 5 | 40510.739279 | • | 3751 | 76907.406192 | 22 | 49.196700 | -8 | 4 | 76499.337570 |
| 3507 | 55270.681753 | [illegible] | 45.190567 | -3 | 4 | 55714.533604 | • | 3780 | 64173.543635 | 83 | 49.199375 | 12 | 13 | 63952.751795 |
| 3507 | 57567.257336 | 44 | 48.187957 | 6 | 4 | 58011.230514 | • | 3780 | 64503.555238 | 20 | 49.199692 | -4 | 13 | 64252.532953 |
| 3513 | 45089.390999 | P | 49.199755 | 11 | 5 | 45551.038613 | • | 3780 | 66435.546548 | 13 | 49.199350 | 3 | 13 | 66214.355466 |
| 3539 | 32529.563905 | [illegible] | 49.204681 | 1 | 5 | 33015.769398 | • | 3948 | 58337.556493 | 96 | 49.200651 | 31 | 4 | 59349.944560 |
| 3539 | 33129.666414 | 16 | 49.204414 | 1 | 5 | 33608.863399 | • | 3948 | 57305.475417 | 205 | 49.200009 | 18 | 4 | 59317.323496 |
| 3549 | 26479.235967 | 14 | 49.205850 | 63 | 5 | 27338.633461 | • | 3900 | 47629.567455 | 9 | 49.202230 | 28 | 14 | 47741.010999 |

REFERENCES


1. Hewish, A., Bell, S. J., Pilkington, J. D. H., Scott, P. F., and Collins, R. A., "Observation of a Rapidly Pulsating Radio Source," Nature, Vol. 217, 1968, p. 709.

2. Pilkington, J. D. H., Hewish, A., Bell, S. J., and Cole, T. W., "Observations of Some Further Pulsed Radio Sources," Nature, Vol. 218, 1968, p. 126.

3. Gold, T., "Rotating Neutron Stars as the Origin of the Pulsating Radio Sources," Nature, Vol. 218, 1968, p. 731.

4. Moffet, A. T., and Ekers, R. D., "Detection of the Pulsed Radio Source CP 1919 at 13-cm Wavelength," Nature, Vol. 218, 1968, p. 227.

5. Bracewell, R. N., The Fourier Transform and Its Applications, McGraw-Hill, New York, 1965, p. 339.

6. Foster, C. F., "Automated Pulsar Receiver," DSN Progress Report 42-20, Jet Propulsion Laboratory, Pasadena, California, April 15, 1974.

7. Slekys, A., A New Pulsar Timer, JPL Technical Report 32-1526, Vol. XIII, Jet Propulsion Laboratory, Pasadena, California, Feb. 15, 1973.

8. Brokl, S. S., "Automated Pulsar Data Collector," DSN Progress Report 42-25, Jet Propulsion Laboratory, Pasadena, California, Feb. 15, 1975.

9. Reichley, P. E., Downs, G. S., and Morris, G. A., "Time-Of-Arrival Observations of Eleven Pulsars," Ap. J., Vol. 159, 1970, p. L35.

10. Cooley, J. W., Lewis, P. A. W., and Welch, P. D., "The Fourier Transform Algorithm: Programming Considerations in the Calculation of Sine, Cosine and Laplace Transform," J. Sound Vib., Vol. 12, 1970, p. 315.

11. Brigham, E. O., The Fast Fourier Transform, Prentice-Hall, Englewood Cliffs, New Jersey, 1974.

12. NBS Time and Frequency Bulletin, U. S. Dept. of Commerce, National Bureau of Standards, Boulder, Colorado, 1968 to 1979.

13. Daily Phase Values and Time Differences, Series 4, U. S. Naval Observatory, Washington, D. C., 1968 to 197[illegible].

14. Times Services Bulletin, Series 11, No. 220, U. S. Naval Observatory, Washington, D. C.

15. Preliminary Times and Coordinates of the Pole, Series 7, No. 210, U. S. Naval Observatory, Washington, D. C.

16. Melbourne, W. G., Mulholland, J. D., Sjorgren, W. L., and Sturms, F. M., Constants and Related Information for Astrodynamic Calculations, 1968, JPL Technical Report 32-1306, Jet Propulsion Laboratory, Pasadena, California, July 15, 1968.

17. Sturms, F. M., Jr., Polynomial Expressions for Planetary Equators and Orbit Elements with Respect to the Mean 1950.0 Coordinate System, JPL Technical Report 32-1508, Jet Propulsion Laboratory, Pasadena, California, January 15, 1971.

18. Moyer, T.D., Transformation from Proper Time on Earth to Coordinate Time in Solar System Barycentric Space-Time Frame of Reference, JPL Technical Memorandum 33-786, Jet Propulsion Laboratory, Pasadena, California, Dec. 1, 1976.

19. Koble, H. M., Pease, G. E., and Yip, K. W., "LS44-An Improved Deep Space Network Station Location Set for Viking Navigation," in Deep Space Network Progress Report 42-35, Jet Propulsion Laboratory, Pasadena, California, Oct. 15, 1976.

20. White, R. J., Rosenberg, A. D., Fisher, P. S., Harris, R. A., and Newhall, N. S., SPACE-Single Precision Cowell Trajector Program, JPL Technical Memorandum, 33-198, Jet Propulsion Laboratory, Pasadena, California, Jan. 15, 1965.

21. Holdridge, D., Space Trajectories Program for the IBM 7090 Computer, JPL Technical Report 32-223, Rev. 1, Jet Propulsion Laboratory, Pasadena, California, September 1, 1962.

22. Taylor, J. H., and Manchester, R. N., "Observed Properties of 147 Pulsars," Astron. J., Vol. 80, 1975, p. 794.